

# How Efficient are Alendronate-Nano/Biomaterial Combinations for Anti-Osteoporosis Therapy? An Evidence-Based Review of the Literature

Joanna Klara <sup>\*</sup>, Joanna Lewandowska-Łańcucka <sup>\*</sup>

Faculty of Chemistry, Jagiellonian University, Kraków, 30-387, Poland

<sup>\*</sup>These authors contributed equally to this work

Correspondence: Joanna Lewandowska-Łańcucka, Email [lewandow@chemia.uj.edu.pl](mailto:lewandow@chemia.uj.edu.pl)

**Abstract:** Osteoporosis is defined as a systemic skeletal disease characterized by low bone mass and microarchitectural deterioration of bone tissue, with a consequent increase in bone fragility and susceptibility to fracture. Because of the systemic nature of osteoporosis, the associated escalation in fracture risk affects virtually all skeletal sites. The problem is serious since it is estimated that more than 23 million men and women are at high risk of osteoporotic-like breakages in the European Union. Alendronate (ALN) is the most commonly prescribed oral nitrogen-containing bisphosphonate (BP) for the prevention and the therapy of osteoporosis. This is also one of the most intensely studied drugs in this field. However, ALN is characterized by restricted oral absorption and bioavailability and simultaneously its administration has serious side-effects (jaw osteonecrosis, irritation of the gastrointestinal system, nausea, musculoskeletal pain, and cardiovascular risks). Therefore, delivery systems enabling controlled release and local action of this drug are of great interest, being widely researched and presented in the literature. In this review, we discuss the current trends in the design of various types of alendronate carriers. Our paper is focused on the most recent developments in the field of nano/biomaterials-based systems for ALN delivery, including nano/microformulations, synthetic/natural polymeric and inorganic materials, hydrogel-based materials, scaffolds, coated-like structures, as well as organic-inorganic hybrids. Topics related to the treatment of complex bone diseases including osteoporosis have been covered in several more general reviews; however, the systems for this particular drug have not yet been discussed in detail.

**Keywords:** osteoporosis, alendronate, drug delivery systems, nanomaterials, biopolymeric formulations

## Introduction

Osteoporosis is one of the most progressive, systemic, and metabolic diseases affecting bone tissue, manifested by a reduction in bone mass and microarchitectural deterioration.<sup>1-3</sup> This is the most common disease of the skeletal system, classified by the World Health Organization (WHO) as a civilization disease.<sup>4</sup> The numbers are terrifying, since one in three women and at least one in six men will experience osteoporotic-like breakages in their lifetime. Reports indicate that over 23 million people in the EU are at high risk of developing osteoporosis. Furthermore, it is also a socio-economic problem, as millions of osteoporotic fractures and related medical treatment/rehabilitation cost European healthcare systems more than 56 billion euro per year (data for 2019). Osteoporosis-related fractures are occurring not only as a result of fragility but also due to the sensory dysfunction, polypharmacy, and impaired balance. Pain, limited mobility, and long-term disability are becoming an indispensable part of patients' lives. Every year in Europe, nearly a quarter of a million people die as a direct consequences of hip or spine fractures caused by osteoporosis.<sup>5</sup>

Current osteoporosis treatments are limited mainly to anabolic agents and anti-resorptive drugs.<sup>6</sup> The anabolic drugs can change bone remodeling, bone modeling, or both of these processes. Most of the anabolic effect in cancellous bone occurs through the remodeling with overfilling of remodeling units. Anabolic agents are expensive, however, they might be dedicated for high-risk patients.<sup>7</sup> The anti-resorptive compounds (eg, bisphosphonates, BPs) restore bone strength by

suppressing the rate of bone remodeling, promoting the completion of bone formation, and reducing the depth of resorption in each of the reduced numbers of bone metabolic units engaged in the remodeling process.<sup>8,9</sup> BPs-based compounds are one of the most commonly used bones targeting agents that might be divided into non-nitrogenous (etidronate, clodronate, tiludronate) and nitrogen-containing compounds (pamidronate, alendronate, zoledronic acid).<sup>10</sup> Bisphosphonates that contain nitrogen are for now perceived as first-line medicines for the treatment of osteoporosis.<sup>11</sup> Among them, alendronate (ALN) is the most frequently prescribed for the prevention and the therapy of postmenopausal osteoporosis, osteoporosis that occurs in men, corticosteroid-induced osteoporosis, and in the treatment of Paget's diseases as well as metastatic bone diseases.<sup>12</sup> Unfortunately being a BCS III drug (high solubility and low permeability due to a polar hydrophilic nature), ALN is characterized by limited oral absorption and bioavailability (0.9–1.8%).<sup>13</sup> The poor bioavailability resulting in the need for the high dosage to be consumed can cause side-effects, mainly for the gastrointestinal tract, associated with oral use. Adverse symptoms include irritation of the upper gastrointestinal tract (dyspepsia, esophagitis, vomiting, nausea, abdominal pain) and osteonecrosis of the jaws (BRONJ).<sup>13,14</sup> Furthermore, oral ALN administration might be associated with serious musculoskeletal pain and cardiovascular risks. Another nitrogen containing BP widely used in treatment of osteoporosis is risedronate (RIS). Although it has higher ability to inhibit FFP synthase<sup>15</sup> compared to ALN, it exhibits a lower affinity to hydroxyapatite.<sup>16</sup> Additionally, it has similar side-effects to ALN due to the oral route of administration. Some studies<sup>17–19</sup> suggest that the treatment with ALN compared to RIS in postmenopausal women resulted in better improvement in the bone mineral density (BMD). Non-orally administrated nitrogen containing BPs already exist in the form of zoledronic acid (ZA), which has a higher binding affinity to bone compared to alendronate.<sup>12</sup> However, when ZA is administrated intravenously, which eliminates side-effects from the gastrointestinal tract, the serious adverse effects such as fever, mild headache, arthralgia, myalgia, flu-like symptoms,<sup>20</sup> and increased risk of atrial fibrillation (AF)<sup>21</sup> might still occur.<sup>22</sup> Intravenous delivery of alendronate was also considered, however the risk of nephrotoxicity, fever, and flu symptoms, as well as electrolyte imbalance,<sup>23</sup> were discouraging, with no superior prevention of vertebral fractures or changes in BMD.<sup>24</sup>

Therefore, the delivery systems enabling controlled release and local action of these drugs while minimizing the systemic side-effects are of great interest, being widely researched and presented in the literature. The aim of this review is to report the current trends in the design of various types of alendronate carriers. We have focused on the most recent developments in the field of nano/biomaterials-based systems for ALN delivery including nano/microformulations, synthetic/natural polymeric and inorganic materials, hydrogel-based materials, scaffolds, coated-like structures as well as organic–inorganic hybrids. All of the reviewed studies are summarized in Table 1, whereas in Figure 1 the discussed herein alendronate carriers are presented.

In many of the drug delivery systems (DDS), straightaway upon their location in the release medium, the initial large amount of drug is released before a stable profile is reached. This phenomenon, called “burst release” in most cases, is undesired due to the toxic side-effects and decreased efficiency of the delivery device. The initial high release rates may lead to supraphysiological levels of drug concentrations near or above the toxic level *in vivo*.<sup>25</sup> Furthermore, the drug released during this stage can be metabolized and excreted before being effectively used. Thus, even if no harm is done this amount of drug is significantly wasted, which is not desirable from both a therapeutic and an economic point of view.<sup>26</sup> Nevertheless, the general difficulty with burst release is its unpredictability, since the amount of burst cannot be considerably controlled. It should be emphasized that, in the case of alendronate, the systems providing a sustainable release and effective local delivery are the most suitable for patients suffering from osteoporosis.<sup>27</sup>

Therefore, the presented review also discusses the various strategies used to prolong the release time/rate and reduce the initial burst release of ALN, including coating/reinforcing with other polymers, drug conjugation, hybrid systems fabrication, etc.

## What Is Osteoporosis and Bone Remodeling?

Since skeletal homeostasis is a complex and highly regulated process, osteoporosis can develop in any situation that affects bone physiology – including genetic, metabolic, hormonal, and immunological disbalances. Primary osteoporosis, also referred to as age-related osteoporosis, is mainly connected to the decline in sex hormones concentration that circulate in the bloodstream. In older men, bone mass reduction occurs at the rate of 0.5–2% per year. When osteoporosis

**Table I** Summary of Articles Included in Literature Review

Structure	Materials	ALN Content	The Release Parameters	Ref.
Polymeric nanoparticles	PCL	Double emulsion technique – highest drug loading – $20.68 \pm 0.66\%$ ; encapsulation efficiency % - The highest $34.31 \pm 0.96\%$ Nanoprecipitation – the highest drug loading – $8.22 \pm 0.29\%$ , encapsulation efficiency % - highest $18.80 \pm 0.7\%$	Longer than 500h – up to even 1900h	[45]
Polymeric nanoparticles	Chitosan	Encapsulation efficiency % – The highest $70.06 \pm 0.05\%$	PBS (pH=6.8) – 42% of the drug released during 360 min; 0.1N HCl – 93% of the drug released during 360 min.	[46]
Polymeric nanoparticles	Chitosan, HA	Encapsulation efficiency % – The highest $75.6 \pm 8.2\%$ Loading capacity % – The highest $38.3 \pm 7.5\%$	Data not presented	[48]
Polymeric nanoparticles	Chitosan	Loading efficiency % – the highest $32.42 \pm 2.02\%$	pH dependent – faster release at acidic pH; 100% of drug released up to 48 hours in pH=7.4; up to 24h in pH=5.8	[49]
Polymeric nanoparticles	Gelatin, glutaraldehyde	Post-functionalization method – 10.8 moles of alendronate linked to one mole of gelatin Simultaneous functionalization method – 17.6 moles of ALN per one mole gelatin	Data not presented	[50]
PLGA nanoparticles	PLGA	DES-E entrapment efficiency – $55.1 \pm 7.4\%$ DES-D – entrapment efficiency – $87.4 \pm 10\%$	90% of the drug released after 4h	[54]
PLGA nanoparticles	PLGA	Conjugation yield – 30–35%	Data not presented	[55]
PLGA nanoparticles	PLGA, $\beta$ -cyclodextrin chitosan, alginate	Drug loading content % – The highest – $54.6 \pm 8.8\%$ Loading efficiency % – the highest – $70.7 \pm 5.6\%$	Up to 72h; for system with highest ALN content after 72h, 75.3% of drug was released	[56]
PLGA nanoparticles	PLGA, chitosan	Drug loading content % – The highest – $76.4 \pm 10.3\%$ Loading efficiency % – the highest – $77.2 \pm 3.1\%$ Conjugation yield – 49.6%	From tested systems - The highest percentage of released ALN during 72h of the experiment – 52.2%, the lowest – 28.8%	[57]
Lipid particles	Glyceryl monostearate, Lutrol 68	Entrapment efficiency % – 74.3%	73% of drug released within 6h	[58]
Lipid particles	Glyceryl monostearate, Tween 80	Entrapment efficiency % – $68.32 \pm 1.64\%$ , drug loading with respect to lipids – 8%, drug content – $97.58 \pm 0.32\%$	Up to 120h; 93.16% of drug released at 102h	[59]
Lipid particles	Polyethyleneimine	Encapsulation efficiency % – The highest – $87.4 \pm 0.7\%$ , loading capacity % – The highest – $23.8 \pm 0.2\%$	Up to 28h; at pH=7.4 total ALN released from the complexes $40.0 \pm 0.1\%$ after 24h, at pH=6.5–23.4 $\pm 0.9\%$	[60]
Liposomes	(DSPC)/ (DSPG), chitosan	Entrapment efficiency % – the highest – $35.4 \pm 3.3\%$ ,	Data not presented	[62]
Liposomes	Phosphatidylcholine (PC), cholesterol (Ch), lecithin (Lec) Eudragit L100, stearylamine (SA), dicetyl phosphate(DP)	Entrapment efficiency % – the highest – 54.16%,	In pH 1.2 – up to 14% of ALN in selected formulation was released in 120 min time frame; in pH 7.4 almost 100% of drug was released within 3h	[63]

(Continued)

Table I (Continued).

Structure	Materials	ALN Content	The Release Parameters	Ref.
Nanotubes	Hydroxyapatite, TiO <sub>2</sub> nanotubes	Drug loading – 4.6 µg/sample TNT-HA	2.1 µg of ALN released after 504 h at pH=7.4 (50% of loaded drug); 4.6 µg of ALN after 12h at pH=4.5 (100% of loaded drug)	[65]
Nanotubes	Carbon nanotubes	Drug loading during synthesis – 0.00625 g/0.1 g MWCNTs	Data not presented	[66]
Nanotubes	Phosphate functionalized (4,4) – armchair carbon nanotubes	Data not presented	Data not presented	[67]
Nanoparticles	Gold	7.32 wt% ALN conjugated to GNPs	Data not presented	[68]
Nanodiamonds	Sp <sup>3</sup> carbon	Data not presented	Data not presented	[69]
Nanocrystals	Hydroxyapatite	ALN attached to nHA – 29.5 wt%, maximum drug surface immobilization – 0.42 mg/mg	Data not presented	[73]
Nanoparticles	Hydroxyapatite, poly(allylamine), alginate	Data not presented	Data not presented	[74]
Microspheres	Nanocrystalline hydroxyapatite, aminated modified polylactic acid (EPLA)	Drug loading – 2.460±0.078 g/g	Drug release rate about 56% in 15 days for AL-loaded EPLA/nHAp composite microspheres in PBS	[77]
Microspheres	Hollow hydroxyapatite	Loading capability – up to 46.8 wt% with respect to the starting materials	Up to ~21 days, after 2 days, drug release ratio – 7%	[78]
Microspheres	PLGA, hyaluronic acid	Encapsulation efficiency % – the highest – 73.52±4.10%	Up to 28 days	[79]
Microspheres	PLGA, PLLA, gelatin	Drug loading – 1.4 mg/g and 2.5 mg/g for M+G+B@ALN (25) and M+G+B@ALN (50)	60% and 50% of loaded drug released during 21 days for M+G+B@ALN (25) and M+G+B@ALN (50)	[80]
Mesoporous silica	Amine modified MCM41, SBA-15	Drug adsorption – 22%, 37%, 8%, 14% for SBA-15-NH <sub>2</sub> , MCM41-NH <sub>2</sub> , SBA-15, MCM41	Up to 300h	[83]
Mesoporous silica	SBA-15 modified with phosphorous group	Drug adsorption – 25.0, 59.1, 87.0 µg/m <sup>2</sup> for SBA-15, P-SBA-15 <sub>HCl</sub> , P-SBA-15	Up to 10 days; after 24h 18.0, 24.2, 34.4 µg/m <sup>2</sup> of drug was released from SBA-15, P-SBA-15 <sub>HCl</sub> , P-SBA-15	[84]
Biosilica	Biosilica	Drug loading – 1.45% w/w	Data not presented	[85]
Mesoporous carbon	Mesoporous carbon doped with nitrogen	Drug loading – 5%	Up to 12h, in pH=1.2, pH=4.5, pH=6.8, pH=7.4–20%, 8–9%, 8–9%, 64% of drug was released correspondingly	[86]
Microspheres	Mesoporous bioactive glass, CaO	Drug loading – 776.83 mg/g	Up to 20 days	[87]
MOF	Phosphonate MOFs with Ca <sup>2+</sup> and Mg <sup>2+</sup>	0.228 g and 0.237 g of ALN per 1 mg tablet for Ca-ALN and Mg-ALN correspondingly	Release rate - 0.26 mmol/min for Ca-ALE and 0.08mmol/min for Mg-ALN. After 192h (240h) 8% (34%) of drug was released for Mg-ALN (Ca-ALN). Two-step controlled released for 480h – 64% and 15% of the drug was released for Ca-ALN and Mg-ALN correspondingly.	[90]
Membrane with MOF	Polycaprolactone, gelatin Zif-8	The 0.5 mg/mL ALN concentration was used during synthesis	5 µg/cm <sup>2</sup> of ALN was released during first 4 days, prolonged release for 21 days	[91]

(Continued)

Table 1 (Continued).

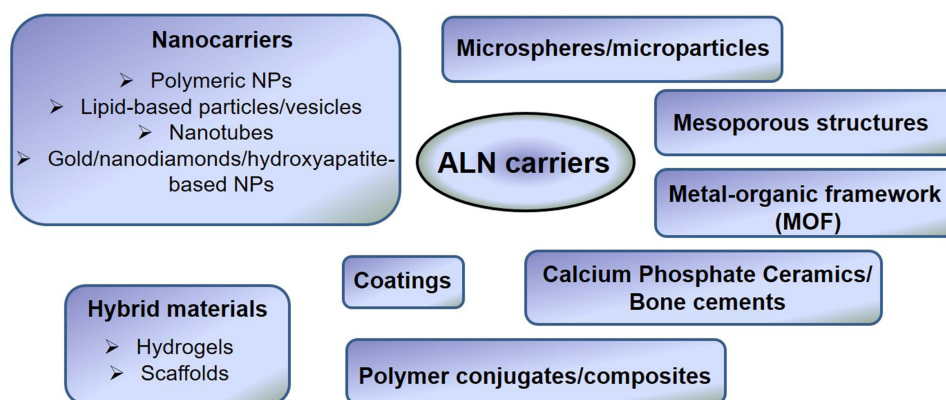
Structure	Materials	ALN Content	The Release Parameters	Ref.
Calcium phosphate	Octacalcium phosphate	Drug content – 5.2 wt%	Up to 50 hours	[96]
Calcium phosphate cement	$\alpha$ -tricalcium phosphate ( $\alpha$ -TCP) cements, gelatin	Maximum ALN concentration 25 mM	Data not presented	[97]
Calcium phosphate cement	Calcium phosphate cement, stearic acid, Precirol ATO5 (Pre), stearic alcohol, cutina HR(Cut) and Tristearin	Encapsulation efficiency% – higher than 90%	Controlled release for at least 21 days	[98]
Calcium phosphate cement	Calcium phosphate cement, PLGA	Drug loaded – 0.5wt% (low ALN dose), 5wt% (high ALN dose)	Negligible release up to 14 days; at 15–42 day of experiment the ALN was released at the dose 0.02/0.2mg per day for low and high ALN dose cement; after 148 days, the amount of released drug reached 0.8mg and 1.2mg for low and high ALN dose cement	[99]
Calcium phosphate scaffolds	Biphasic calcium phosphate	Drug loading – 786.28 $\pm$ 6.68 $\mu$ g in ALN (1 mg)/BCP scaffold; 3638.49 $\pm$ 7.12 $\mu$ g in ALN (5 mg)/BCP scaffold	During 28 days, 72.42 $\pm$ 1.01%, 19.36 $\pm$ 0.16 of ALN was released from ALN (1mg)/BCP scaffold and ALN (5mg)/BCP scaffold respectively	[100]
Coating	4-azobenzoic acid-chitosan	Drug loading – 293.84 $\pm$ 8.04 $\mu$ g/plate (73.46 $\pm$ 2.01 $\mu$ g/coating)	15.56 $\mu$ g/day during first week, and 2.6 $\mu$ g/day for 56 days	[103]
Coating	Octacalcium phosphate, titanium	Drug loading – for AL8 – relative content of CaAL $\cdot$ H <sub>2</sub> O – 48wt%	Data not presented	[104]
Coating	APTES, glutaraldehyde, titanium	Drug immobilized – Method 1 – the highest – 1186 $\pm$ 36 ng/cm <sup>2</sup> ALN-P-Ti-2.5 (5); method 2 – the highest 1655 $\pm$ 32 ng/cm <sup>2</sup> and ALN-S-Ti-1	33% and <10% of drug released from ALN-P-Ti-2.5 (5) and ALN-S-Ti-1 after 14 days	[105]
Coating	Hydroxylated TiO <sub>2</sub>	Data not presented	Data not presented	[106]
Coating	Magnesium doped hydroxyapatite, PCL	Drug loading during synthesis – 200 $\mu$ g/sample	34% and 26% of ALN was released after 24h for samples with 2 and 4% PCL coating, with no coating – 75% of ALN was released during 12 hours.	[27]
Polymer conjugate	D-aspartic acid octapeptide, N-(2-hydroxypropyl)-methacrylamide (HPMA) copolymer, MA-GLY-GLY-Pro-Nle-OH	Drug content – up to 8.5 mol%	Data not presented	[109]
Polymer conjugate	EP4, Leu-ARG-PABA	Data not presented	5 $\mu$ g/kg/day with 5 day half time	[110]
Polymer conjugate	Fmoc-Phe-Phe	Data not presented	Data not presented	[111]
Hydrogels	Gellan gum, PLGA	Encapsulation efficiency% – 70.3 $\pm$ 0.49%, loading efficiency% – 5.1 $\pm$ 0.6%	16 $\pm$ 3 $\mu$ g of ALN every 5 days; after 25 days, 8% of drug was released	[116]
Hydrogels	Chitosan, $\beta$ -glycerol phosphate disodium salt pentahydrate	ALN concentration – 2, 5, 10 mg/mL	Prolonged release up to 30, 45 and 65 days for system with 2,5,10mg/mL ALN	[23]
Hydrogels	Silica	Drug loaded – 0.5 g/0.66 g	Up to 144h (data for ETID, PAM); after 48h ~70% of ALN was released from gel	[117]
Hydrogels	Tetra-PEG	Data not presented	Up to 28 days; 20% of ALN was released during first 4 days	[118]

(Continued)

**Table I** (Continued).

Structure	Materials	ALN Content	The Release Parameters	Ref.
Hybrid hydrogel	Silica, collagen/chitosan/hyaluronic acid	Drug loading – 3.3% (TG), 6% (UV-Vis)	56% of drug after 168h	[119]
Scaffolds	Poly (L-lactide-co-ε-caprolactone), bioactive glass-ceramic	The entrapment efficiency% – 11.5% and 14% for initial 50 mg and 100 mg drug	Up to 48h	[120]
Scaffolds	PCL	Drug loading – 84.6±5.5 µg/scaffold for ALN (1wt%)/PCL and 471.6±10.2 µg/scaffold for ALN (5 wt%)/PCL	Over 28 days, 95.2±1.2µg ALN was released for ALN (1 wt%)/PCL and 389.2±5.4µg ALN for ALN (5 wt%)/PCL	[121]
Hybrid hydrogel	Hydroxyapatite, collagen	Drug content – 4.0 wt%	Data not presented	[125]
Scaffolds	Alginate, nanobioactive glass, calcium, copper	Encapsulation efficiency% – 98.7±0.1%	After 2 months, 76±5µg/mL (89±4% of total amount) of ALN was released from AlgNbgCu/ALN scaffolds; after 2 months 48±9µg/mL (56±11% of total amount) of ALN was released from AlgNbgCa/ALN scaffolds	[126]
Scaffolds	Chitosan, nanohydroxyapatite, PLLA, nanohydroxyapatite	Data not presented	Sustained release for up to 30 days for PLLA/nHA scaffolds with CH/nHA-ALN	[127]
Scaffolds	Tricalcium phosphate, PCL	Drug loading during synthesis – 500, 800, 1,000 µg/scaffold	Up to 168h for 1% PCL coated scaffold at pH=7.4 and pH=5.0; up to 168h for non-coated scaffold at pH=7.4 and up to 70h for non-coated scaffold at pH=5.0; higher release in more acidic medium	[128]
Scaffolds	Graphene oxide, collagen	Drug loading rate – 45.40±3.12% and 48.12 ±1.99% for Col-0.05% GO-ALN and Col-0.2% GO-ALN sponge	Up to 30 days, slower release from Col-0.2%GO-ALN sponge	[129]

occurs in older women as an effect of deficiency in estrogen around the time of menopause, the postmenopausal osteoporosis term can also be used.<sup>28</sup> The limited concentration of estrogen allows for the upregulation of the production of RANKL (Receptor Activator for Nuclear Factor κ B Ligand), which is responsible for osteoclast differentiation and as a result the bone resorption. However, a decrease in sex hormones concentration is not the sole factor that causes osteoporosis development. During aging, as a result of oxidative stress, shortening of telomeres and weakening of DNA repair mechanisms, the cell aging occurs, which is associated with a decrease in the differentiation of osteocytes and osteoblasts, changes in the stiffness and quality of the bone matrix. Secondary osteoporosis refers to cases when this disease is developed as a consequence of other illnesses or medication. It should be emphasized that skeleton

**Figure 1** The selected delivery systems of alendronate.

homeostasis is connected to the regulation of other organ systems. Moreover, the secondary factors (lifestyle, disease, medications) can also be the explanation for osteoporosis occurrence.

Bone quantity and quality influence skeletal strength as well as the resilience to fracture. Factors, that determine the bone quantity include peak bone mass, rate, and degree of bone loss, while bone quality is connected with the bone matrix and micro/macrostructure conditions. Osteoporosis is strictly related to changes in these determinants and is developed when the proper balance between the bone formation (osteoblasts) and bone resorption (osteoclasts) that occurs during bone remodeling is disrupted.<sup>29</sup> The first step in the remodeling process is bone resorption. A microcrack causes the break in the continuity of canaliculi, which affects osteocytic apoptosis, with the location and extent of the damage defined by signals to lining cells (osteoblasts in the rest state). Lining cells and osteocytes release local factors that are a signal for osteoclast precursor cells to migrate into the remodeling compartment and differentiate in osteoclasts (osteoclastogenesis). Osteoclasts resorb the matrix and the microcrack – this resorption phase lasts about 2–4 weeks and ends with osteoclast apoptosis. After this period, there is a short retreat phase, in which the resorptive cavity becomes lined with bone-forming cells (osteoblasts). Osteoblasts produce an osteoid (bone formation phase), which is gradually mineralized. After about 4–6 months, the bone metabolic unit (BMU) is filled with fully mineralized bone. Osteoblasts trapped within the newly-formed bone matrix transform into osteocytes, others die or form new, flattened osteoblast lining cells.<sup>8,30</sup>

In the pathomechanism of osteoporosis, as a result of loss of control over the functioning of bone cells and/or communication between them, the resorption and bone formation processes are decoupled. This cause an increase in resorption and acceleration of bone turnover. When the bone formation is lower than bone resorption, each remodeling event removes a small moiety of bone from the skeleton. This leads to bone loss and structural damage, which further enhances the increased turnover of bone (more resorptive cavities on a given surface at a given time, shorter mineralization time).<sup>31</sup> The rapid remodeling is associated with an increased risk of fracture since densely mineralized bone is removed and replaced with less densely mineralized one. As a result of reducing material, bone may become too flexible and crack under usual loading conditions.<sup>32</sup> Furthermore, the delay in the initiation and slower completion of bone formation mean that the excavated resorption sites remain temporarily unfilled, creating stress concentrators that predispose a bone to microdamage. Finally, it was also reported that increased remodeling modifies isomerization and maturation of collagen, which also increases the fragility of bone.<sup>33</sup>

Remodeling activities of a basic multicellular unit composed of osteoclasts and osteoblasts are coordinated by osteocyte cells that occur in the bone matrix. A schematic representation of bone resorption and formation is presented in Figure 2. Osteoclasts activation is initiated by humoral stimuli and mechanical loading and, therefore, several factors can contribute to the development of osteoporosis. Among them, impairment of Runt-related transcription factor 2 (Runx2) activity might obstruct the differentiation of osteoblast by promoting the formation of adipose cells from mesenchymal stem cells. Additionally, an increase in DKK-1 (dickkopf-related protein I) and sclerostin, which are

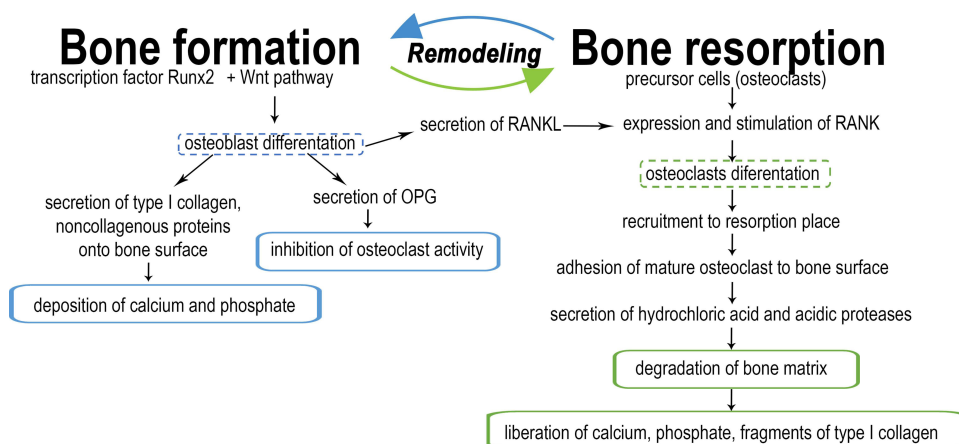


**Figure 2** The schematic representation of bone formation and resorption.

antagonists of the Wnt pathway, can suppress the formation of new bone. The regulation of the remodeling process is conducted mainly by osteocytes. Expression of surface receptors for PTH (parathyroid hormone) and Wnt, as well as secretion of RANK and OPG (osteoprotegerin), ensure proper bone remodeling. Mechanical loading of osteocytes leads to activation of Wnt, downregulation of RANKL, and inhibition of sclerostin which results in osteoclast inhibition and osteoblast differentiation; the mechanical unloading causes reciprocal changes. Furthermore, by osteocyte apoptosis, triggered among others as a result of estrogen withdrawal, local bone microdamage, and oxygen deprivation, bone resorption is promoted through the recruitment of osteoclasts. Alteration of the ratio of RANKL and OPG can lead to disruption of the balance between bone formation and resorption. Both the RANKL increase and OPG decrease are facilitated by the decrease in estrogen concentration. Discontinuous, cyclic elevation in PTH concentration allows for stimulation of bone formation, however, when raised PTH concentration is sustained, production of RANKL and M-CSF (Macrophage colony-stimulating factor) is increased, which in turn promotes bone resorption.<sup>20,34</sup>

## Alendronate – Its Uniqueness and Limitations

The idea of using bisphosphonates (analogs of inorganic pyrophosphates) as medicines for osteoporosis was raised in the 1960s when the first research about the biological effect of this group of compounds emerged.<sup>35</sup> These compounds contain two phosphonate groups sharing a common carbon atom in their structures known as P–C–P backbone.<sup>36,37</sup> Chemically, BPs are analogous to pyrophosphates, which have been shown to be naturally occurring modulators of bone metabolism.<sup>38</sup> Pyrophosphate is characterized by P–O–P backbone and is known to have a strong affinity to apatite crystals while being prone to acidic/enzymatic hydrolysis. On the contrary, P–C–P bonds of BPs are far more stable while maintaining their affinity towards the apatite. The two phosphonate groups are essential for both binding to hydroxyapatite (HAp) and for the biochemical mechanism of action. The two remaining R<sup>1</sup> and R<sup>2</sup> groups on the carbon atom of the P–C–P backbone can further modulate the affinity of the BPs towards apatite.<sup>39</sup> For example, when R<sup>1</sup> is a hydroxyl group the enhancement of the ability of the BPs to attach to bone mineral surface, and prevention of dissolution of hydroxyapatite was observed due to the formation of a tridentate bond, which was superior in forming chelate calcium ions to the bidentate binding. Whereas the R<sup>2</sup> side group has some effect on binding but predominantly determines the antiresorptive potency of the BPs. In particular, the R<sup>2</sup> side chain of nitrogen-containing BPs can also influence overall bone affinity as a result of the ability of the nitrogen moiety to interact with the crystal surface of bone mineral.<sup>40</sup> The positive charge of this group increases its affinity towards negatively charged phosphonate groups due to the electrostatic interactions. For maximal potency, the presence of a nitrogen atom in R<sup>2</sup> chain is required, and the distance from the P–C–P group and spatial configuration must be appropriate.

Alendronate (ALN) in the form of alendronate acid is an example of nitrogen-containing bisphosphonates. Free amine moiety present in its structure can form a hydrogen bond with a hydroxyapatite surface. The presence of nitrogen groups within the R<sup>2</sup> side group is associated with the ability to inhibit farnesyl pyrophosphate (FPP) synthase, a major enzyme in the mevalonate pathway. As a result, many of the activities of the osteoclasts are disrupted, including migration, attachment, resorption, and, ultimately, cell death can occur via apoptosis.<sup>41</sup> The schematic representation of nitrogen-containing bisphosphonates' interaction with bone is depicted in Figure 3, while the mechanism of action at the cellular level is reviewed in Figure 4.<sup>35–37,42</sup> Briefly, alendronate inhibits farnesyl PP synthase which leads to not only inhibition of the creation of geranyl pyrophosphate (GPP) and farnesyl pyrophosphate (FPP), but also, as a result, it inhibits the formation of cholesterol and prenylated small G-proteins, because both geranylgeranyl pyrophosphate (GGPP) and FPP are involved in their post-translational prenylation. The lack of these compounds leads to dysregulation of cells processes, which in turn causes osteoclasts dysfunction. Thus, ALN acts by inhibiting the resorptive activity of mature osteoclasts causing their apoptosis.

Alendronate has 10–1000 relative antiresorptive potency via oral delivery compared to etidronate.<sup>37</sup> As mentioned above, ALN is characterized by limited oral absorption and bioavailability.<sup>13</sup> The reason behind the low absorption of BPs administered orally is that physiologic pH in the intestine causes ionization of alendronate and its weakly lipophilic nature which causes that absorption is mainly performed by paracellular transport.<sup>36</sup> The dosage and frequency of administration vary with sex and whether it is used for treatment or prevention. Side-effects are mainly associated with challenging and specified ways of administration – with water, 30–60 minutes before the first meal, and any meal liquid

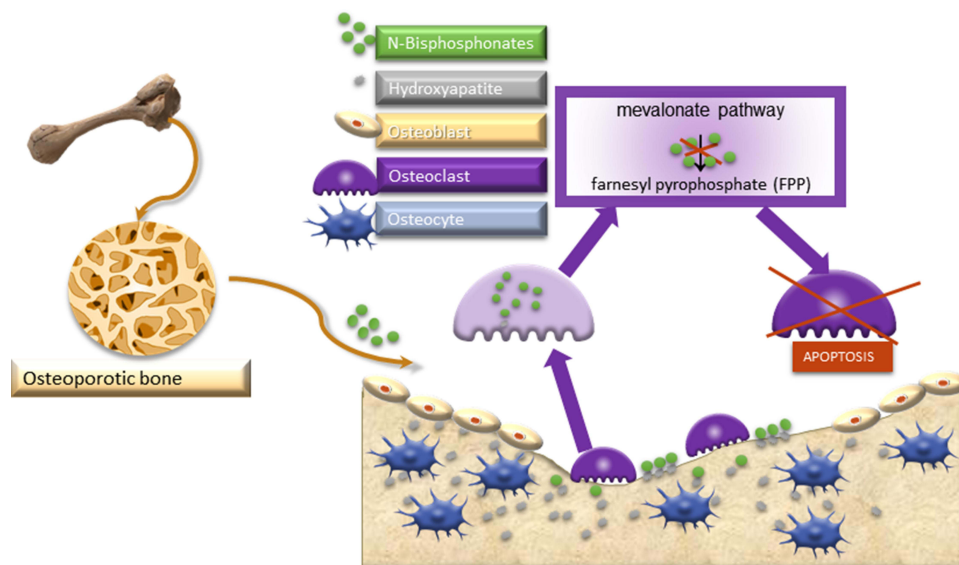


Figure 3 The schematic representation of nitrogen-containing bisphosphonates' interaction with bone.

## Alendronate mechanism of action

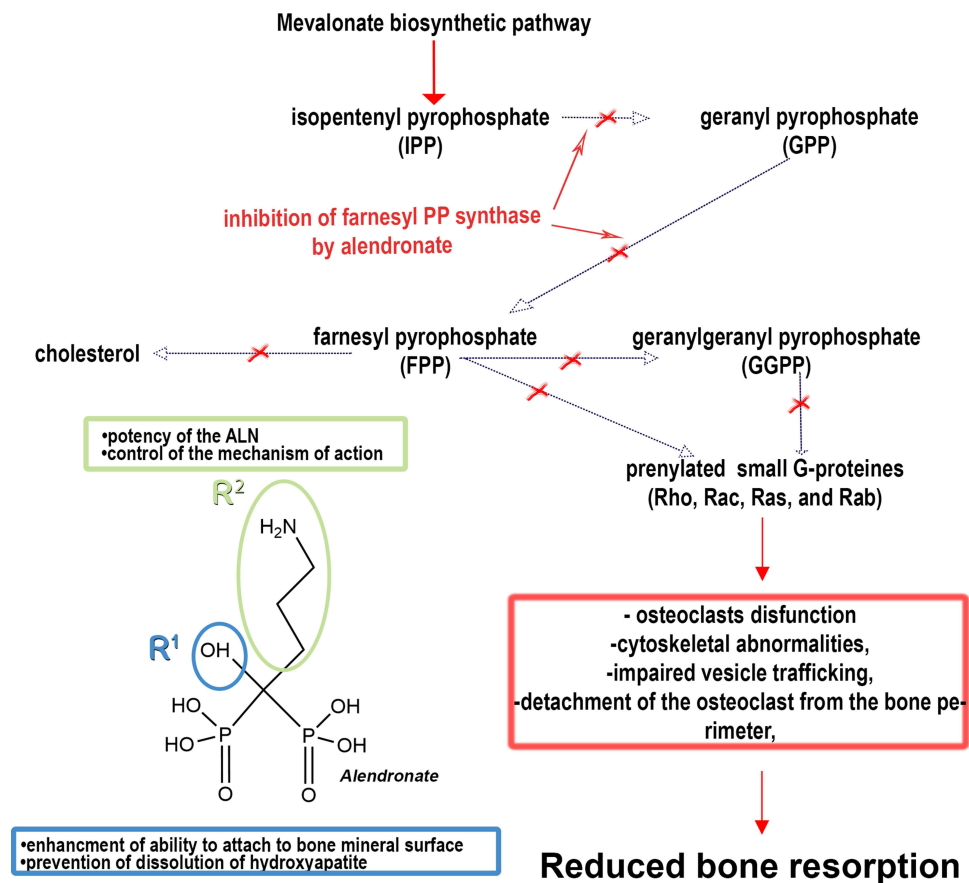


Figure 4 The scheme of alendronate mechanism of action.

or solid, which contains divalent metal ions, should be ingested only 2 hours after the drug intake. These requirements are necessary to restrain any further decrease in absorption and bioavailability.<sup>37</sup> It should be stressed that bisphosphonates have a strong affinity to divalent ions resulting from their chelation by BPs. The formed complexes with  $Mg^{2+}$  or  $Ca^{2+}$  are even less absorbable; therefore, patients should avoid meals containing these components close to the drug ingestion to not fully block the bioavailability of ALN. Additionally, it is advised to stay up for a minimum 30 minutes after drug administration to prevent esophagitis. Although effectiveness in hip, forearm, and spine fracture prevention was shown, undesirable effects unfortunately occur.<sup>43</sup>

Alendronate, as a nitrogen-containing bisphosphonate, is not metabolized in the body. The route of excretion of ALN is by the kidney with urine. Still, about 40–60% of this compound is being preserved in bone – terminal half-life ~ 200 days.<sup>13,37</sup> After approximately 3 months of oral treatment, activation of inhibition of bone resorption should be achieved.<sup>37</sup> However, bisphosphonates distribution, such as alendronate, is not uniform – it was found that uptake in areas of active bone remodeling and resorption and in the spine is higher in comparison to the femoral shaft.<sup>36</sup>

## Nanocarriers for ALN Delivery

Nanotechnology is currently widely used in the medical field. Nanostructures can be employed as carriers for proteins, enzymes, genes, and vaccines as well as for drugs. Conventional methods for medicine delivery include the enteral and parenteral route of drug administration. Even though the first mentioned path is preferred due to its non-invasive nature, the drug absorption and bioavailability are limited. Nanocarriers could not only help to prevent these drawbacks but also facilitate sustained release, improve/intensify the pharmacological response, and decrease/minimize side effects. By using these structures, which usually should be less than 200 nm in diameter due to the size of microcapillaries in the body, increased stability, solubility, biodistribution, pharmacokinetics, and reduced toxicity, prolonged and targeted drug delivery can be achieved.<sup>44</sup>

## Polymeric Nanoparticles (NPs)

Polymeric nanoparticles that are fabricated from the natural or synthetic biodegradable polymers can entrap drugs in their core or matrix. They effectively penetrate the cell membrane, have good stability in the bloodstream and the ability to carry a high drug concentration. The additional advantage of these types of nanostructures is that they can maintain the stability of the volatile pharmaceutical agent. The drug can also be absorbed on their surface. Monomers, which are the product of biodegradation of polymeric nanoparticles, can be degraded via metabolic pathways. Importantly, changes in the physicochemical properties of polymers can facilitate enhancement in controlled release.<sup>44</sup>

Miladi and coworkers presented the polycaprolactone (PCL)-based nanoparticles loaded with alendronate<sup>45</sup> employing two strategies – double emulsion evaporation (DEV) and nanoprecipitation. For both methods nanoparticles with sizes in the range of 195–447 nm and negative zeta potential (from –10.3 mV to –0.53 mV) were obtained. However, higher encapsulation efficiency was recorded for the double emulsion technique (15.12–34.21%) compared to nanoprecipitation (0.36–18.8%), which could be related to the weak interaction between used polymer and alendronate. Release profiles obtained for selected formulations from DEV method showed that ALN undergoes sustained release even up to 18:00 hours when a high molecular weight polymer is used for nanoparticles formulation. Additionally, burst release was significantly more noticeable in the case of nanoparticles formed by nanoprecipitation.

Later work of the same authors<sup>46</sup> focused on the incorporation of ALN into chitosan nanoparticles without the usage of organic solvents like acetone or dichloromethane, which are inappropriate for pharmaceutical products and, thus, should be limited. Since chitosan is a naturally occurring polysaccharide, it does not show toxicity and might be degraded in the physiological environment.<sup>47</sup> Additionally, the positive charge of chitosan that allows for interaction with mucin via electrostatic forces may be advantageous for ALN delivery, which is poorly absorbed. The authors prepared nanoparticles by ionic gelation technique with polyanions like sodium tripolyphosphate (TPP) in an oil emulsion. All obtained nanoparticles had a positive potential zeta charge in the range between 21 and 27 mV and a size below 200 nm. Encapsulation efficiency varied between 50% and 70%, which is significantly higher compared to their previous work, and thus could indicate that the application of ionic gelation technique chitosan-based NPs is superior for ALN incorporation. Revealed *in vitro* release profiles were different for 0.1 M HCl and PBS medium (pH=6.8). In the case

of the latter, prolonged equilibrium time (240 min) was observed and after 360 min only 42% of encapsulated ALN was released. Another approach for alendronate delivery in the chitosan-based NPs was presented by Dong et al.<sup>48</sup> Together with ALN the curcumin (CUR), which is showing the bone regenerating activity, was incorporated into resulting vehicles and co-delivered at the same time. Additionally, nanoparticles were coated with hyaluronic acid (HA), a polysaccharide very often used in tissue regenerating and wound healing. This nano-delivery system was prepared by the high-pressure homogenization-solvent evaporation technique. The results revealed the significant impact of the alendronate to curcumin ratio on the particles sizes and zeta potential values. The mean particle size increased from 172 nm (ALN/CUR ratio=1:1) to 372 nm (ALN/CUR ratio=1:5) and the reverse tendency was observed for zeta potential – a decrease from +43 mV to +31 mV. For a higher ALN/CUR ratio, the entrapment efficiency for alendronate increased and reached the maximum value of about 76%. Coating with hyaluronic acid resulted in the growth of mean particle size, %EE, %LC, and reduction of zeta potential, with a higher concentration of HA. Bone regeneration efficiency in vitro tests performed on MC3T3-E1 cells confirmed that developed NPs effectively induce mineralization and support the cells proliferation. Furthermore, up-regulation of osteocalcin (OCN), bone morphogenetic protein (BMP-2), and Runx2 were also revealed.

Further research involving the use of chitosan for ALN delivery was conducted by Moradikhah et al.<sup>49</sup> Fabricated by the means of the cross-junction microfluidic devices structures were in the range 102–215 nm, and their zeta potentials were between  $\pm 21$  to  $\pm 28$  mV, which was similar to the parameters obtained in the previously mentioned work.<sup>46</sup> The diameters of developed nanoparticles determined utilizing SEM, AFM, and DLS techniques were in good agreement. The higher concentration of alendronate and the lower flow rate allowed to achieve the highest value of the loading efficiency for all tested compositions (32.42% $\pm$ 2.02). The authors found that, in a more acidic medium, the total release occurred faster (24 h) compared to neutral pH (48 h). In vitro studies of human adipose stem cells (hA-MSCs) revealed higher OPN and ALP mRNA levels when compared to control after 2 and 3 weeks of culturing, thus demonstrating the osteogenic potential of developed systems.

In another work,<sup>50</sup> glutaraldehyde-crosslinked gelatin nanoparticles were employed as an alendronate delivery system. Biocompatibility, nontoxicity, biodegradability, and tunability, in addition to low cost, make gelatin ideal material for biomedical application.<sup>51</sup> The main aim of this study was to fabricate the mineral-binding nanostructures that would have the ability to enhance an affinity to the bone mineral ( $\text{CaPO}_4$ ). A two-step desolvation method was executed for gelatin nanoparticles formation and glutaraldehyde was used as a crosslinker. The authors presented two different approaches for alendronate conjugation – during the crosslinking reaction and 16 hours after aging. Although SEM analysis did not show any significant changes in resulting products, the DLS measurements revealed that NPs had a larger size in the swollen state when they were functionalized simultaneously, which was in turn confirmed by cryo-TEM. For Gel-ALN nanoparticles, after 7 days of soaking, 70 wt% of alendronate was retained. In non-functionalized gelatin NPs, less than 5 wt% initially bound alendronate was present after the same time frame. Overall authors demonstrated that functionalized with ALN gelatin-based NPs possess higher calcium phosphate affinity. One of the most enthusiastically studied polymers for drug delivery is copolymer poly (lactic-co-glycolic acid) (PLGA) which is an example of synthetic biodegradable material approved by the United States Food and Drug Administration, European Medicine Agency, and other federal agencies, owing to its biodegradability, biocompatibility, and immune neutral features.<sup>52</sup> Due to its biocompatibility, tunable degradation rates, and nontoxicity, it is a popular choice in the formation of nanoparticles for biomedical applications.<sup>6,53</sup> Changes in particle size, porosity, copolymer ratio, molecular weight, and synthesis conditions can provide appropriate alterations in drug release profiles. Cohen-Sela et al.<sup>54</sup> employed the double emulsion solvent diffusion (DES-D) technique to encapsulate alendronate into PLGA nanoparticles. Obtained results were compared with the classical double emulsion solvent evaporation technique (DES-E) which was demonstrated as a method for encapsulation of ALN earlier by Miladi et al.<sup>45</sup> Experimental studies showed that DES-D method allowed for the formation of smaller nanoparticles (~145 nm) with higher ALN entrapment efficiency (~87.4%). To overcome the high solubility of alendronate in water, the authors proposed the introduction of calcium ions, which was essential for the enhancement of drug entrapment. However, the complete release of the drug was observed after 4 hours. RAW 264 cells proliferation inhibition was significantly higher for ALN-NPs in comparison to free ALN and this effect was slightly more pronounced for nanoparticles prepared by DES-D method. Finally, in vivo studies carried out on rabbits have shown that the developed NPs effectively protect the drug in the circulation for a time adequate for

absorption by monocytes, while allowing for sufficient release of ALN inside the cells. In a work by Cenni et al,<sup>55</sup> the PLGA-alendronate conjugate-based nanoparticles were presented. ALN was covalently bound to PLGA, containing a free end carboxylic group in the presence of N'-(3-dimethylaminopropyl)-N-ethyl carbodiimide hydrochloride (EDC) initiator. Nanoparticles were synthesized by emulsion/solvent evaporation technique, and their mean size was ~199 nm. Additionally, the zeta potential of conjugates was -37.2 mV, which was close to the value found for pure PLGA nanoparticles (-41.7 mV). Performed *in vitro* tests revealed the lack of cytotoxicity, hemolytic effect, and platelet release reaction caused by prepared nanoparticles. Although synthesized structures influenced coagulation, the authors concluded that these changes should not be clinically significant. Jing and coworkers<sup>56</sup> developed alendronate-decorated NPs synthesized through ionic cross-linking between PLGA,  $\beta$ -cyclodextrin-modified chitosan (PLGA-CS-CD), and ALN-modified alginate (ALG-ALN). In this approach  $\beta$ -cyclodextrin (CD) was first conjugated to chitosan using maleic anhydride as a linker and next PLGA was grafted to resulted CS-CD through the amide reaction. The prepared PLGA-CS-CD/ALG-ALN NPs were negatively charged and their DLS-average size was between 300–500 nm. The authors demonstrated that ALN release from the nanoparticles might be adjusted by playing with the polymer ratio. *In vitro* biological experiments on MC3T3 cells showed that the nanoparticles had good cytocompatibility. Moreover, the hemolysis test revealed their good blood biocompatibility with low hemolysis ratios (<5%). Finally, it was demonstrated that fabricated PLGA-CS-CD/ALG-ALN NPs exhibited a significant higher binding ratio to HAp disks compared with control system without ALN modification. Recently also the bone-targeted polymeric NPs for ALN delivery based on PLGA conjugated chitosan (CS-PLGA) and alendronate conjugated PLGA (ALN-PLGA) were presented.<sup>57</sup> Both conjugates were obtained employing EDC/NHS chemistry. Developed NPs exhibit sizes in the range of 200–300 nm and reveal sustained ALN release. The authors used a similar methodology as in their previous work discussed above and *in vitro* studies confirmed good cytocompatibility of the NPs against MC3T3 cells while, in the HAp affinity test, a significantly higher binding ratio to HAp disks for ALN-modified NPs was demonstrated.

## Lipid-Based Particles and Vesicles

Lipid-based particles are suitable nanocarriers for lipophilic drugs. Commonly they are composed of glycerides (mono, di, tri), free fatty acid and alcohols, steroids, or waxes which facilitate a solid form of this type of lipids at room temperature. Typical delivery for these nanocarriers is through oral, parenteral, and topical administration. Medicine could be incorporated into the matrix, core, or shell of the lipid particles due to the fact that the first preparation step is to disperse melted solid lipid in the water and stabilize it with emulsifiers. One of the greatest disadvantages of lipid particles is their low drug loading capacity and burst release. However, it can be overcome with new generation lipid particles – a mixture of solid lipid and liquid lipid.<sup>44</sup>

Hosny and Santos<sup>58</sup> presented a study on the enteric-coated solid lipid nanoparticles as a novel ALN delivery system that overcomes low bioavailability and side-effects of orally administered pure drug. By enteric coating, the delivered drug is protected from disintegration in the stomach and its larger amount stays in intact form and is transferred to the small intestine. Loading of ALN into solid lipid nanoparticles was performed by the solvent injection technique. In the optimization process, the NPs composed of glyceryl monostearate as a core lipid at 30% w/w were selected with Lutrol 68 at 5% w/w to achieve an entrapment efficiency of about 74%. The size of homogenous, spheroid nanoparticles verified by DLS measurement was approximately 100 nm. Importantly, after 90 days of storing at 4°C, the size of developed systems did not change. Evaluation of drug release from NPs was compared to the Fosamax tablet. At pH=1.2, which corresponds to the enteric environment after 2 h, only 5% of alendronate was released from nanoparticles, but 85% from tablets. These findings were also confirmed by *in vivo* tests in rabbits – maximum plasma concentration was higher for nanoparticles (~16.54 ng/mL) than for tablets (4.92 ng/mL). Furthermore, ALN absorption was longer when the drug was released from NPs. Das et al<sup>59</sup> developed an interesting ALN delivery carrier by combining Solid Lipid Nanoparticles (SLN) with thermosensitive injectable sol-gel systems. For alendronate-loaded SLN, high-pressure homogenization was employed, and similarly as in the preceding work, glyceryl monostearate was selected as the core lipid with Tween 80 as a surfactant. Prepared SLN was characterized for particle size (222±4 nm), entrapment efficiency (about 68%), and zeta potential (-32 mV). SLN dispersion was next entrapped in the entangled polymeric network of pluronic triblock copolymer. The authors demonstrated that developed systems exhibit gelation time varied within the

range of 41–55 seconds under a temperature between 24.9–33.2°C. A further test proved that the prepared materials were syringeable via an 18 gauge needle and exited the syringe after 7.61–12.24 seconds. Prolonged drug release in situ was confirmed by *in vitro* tests showing that, for the optimized formulation, 93.16% of the entrapped drug was released by 102 h. The *in vivo* studies performed on Wistar rats revealed that no morphological changes and no infiltration of inflammatory cells were observed for the tested formulation. The alternative DDS, based on the ALN-polyethyleneimine (PEI) ion-pairs incorporated into nanostructured lipids (NCLs) utilizing a solvent injection method, was proposed by Abd El-Hamid et al.<sup>60</sup> The schematic representation of ALN/PEI-containing nanostructured lipid carriers (NLCs) formation is illustrated in Figure 5. Association complexes were formed at pH=5 and the most favorable stoichiometry was estimated at a 6.6:1 PEI/ALN molar ratio. It was found that NLCs encapsulated with alendronate/PEI complexes exhibit smaller sizes, higher zeta potential, and significantly higher loading capacity compared to pure alendronate in lipid carriers. Two different pH conditions were employed for drug release experiments, namely pH=6.5 and pH=7.4. For ALN-loaded lipid carriers change in pH buffer did not significantly influence the cumulative drug release during 24 h, whereas for alendronate/PEI complexes a two times higher amount of drug was released in higher pH. Nonetheless, when comparing the kinetics of ALN release at pH=6.5 it was revealed that, after 24 h, ALN/PEI-lipid carriers released only 1/3 of the ALN amount compared to ALN-NLCs.

Both types of molecules – hydrophilic and hydrophobic – can be delivered by the means of liposomes being the spherical vesicles with lipid bilayer membranes and aqueous interiors. Inside the aqueous core the hydrophilic medicine might be dissolved while, in the lipid bilayer hydrophobic molecules can be transported. By changing the type and/or content of lipid molecules building liposomes, their properties including permeability can be adjusted.<sup>6</sup> Liposomes possess many unique features such as low toxicity and biodegradability. When drugs are incorporated into liposomes, their pharmacokinetics and biodistribution are improved.<sup>44</sup> Nevertheless, it should be noted that liposomes exhibit short circulation half-life<sup>6</sup> and low stability during storage that leads to the uncontrolled leakage of the

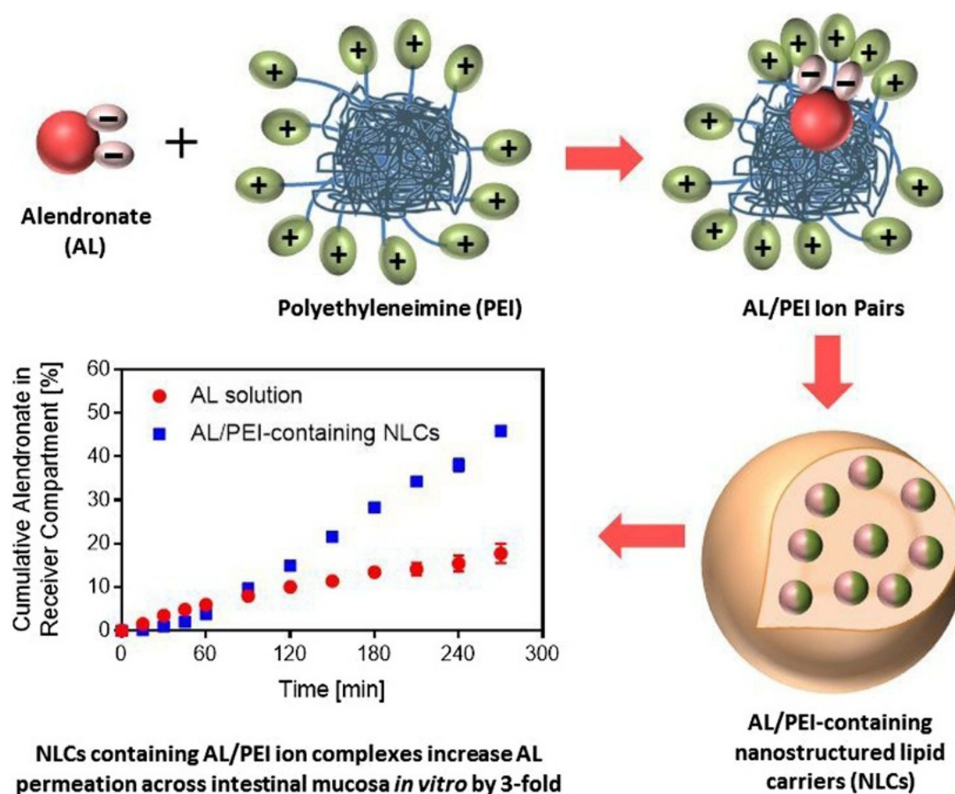


**Figure 5** The graphical abstract with a schematic illustration of the formation of AL/PEI-containing nanostructured lipid carriers (NLCs).

**Note:** Reprinted from Abd El-Hamid BN, Swarnakar NK, Soliman GM, Attia MA, Pauletti GM. High payload nanostructured lipid carriers fabricated with alendronate/polyethyleneimine ion complexes. *Int J Pharm.* 2018;535(1–2):148–156. Copyright (2018), with permission from Elsevier.<sup>60</sup>

entrapped drugs, thus substantially limiting the application of pure liposomes. Various approaches have been proposed to overcome the stability limitations and to improve the liposomes retention in the blood.<sup>61</sup> Han et al<sup>62</sup> presented a liposomes-based system for ALN delivery obtained by modified thin-film hydration method with use of 1,2-distearoyl-sn-glycero-3-phosphocholine (DSPC)/1,2-distearoyl-sn-glycero-3-[phosphor-rac-(1-glycerol)] (sodium salt) (DSPG) and additionally coated with chitosan by electrostatic interactions. Coating with chitosan did not significantly change entrapment efficiency, however, the size of liposomes increased almost three times, and the zeta potential changed sign from  $-32$  mV (uncoated liposomes) to  $+35$  mV. The model in vitro studies revealed that at higher pH=10, during the 24 h incubation period, 23% and 17% of alendronate was released from uncoated and coated liposomes, respectively. When considering stability in the medium with lower pH=2, only negligible drug release was observed from both formulations. In regard to long-term stability at 25°C it was found that coated liposomes decreased their size and zeta potential, but no apparent drug leakage in comparison to uncoated liposomes was revealed. Importantly storing these structures at 4°C or in the freeze-dried state could be conducted up to 3 months with no significant changes in particle characteristic or amount of encapsulated drug. By employing Caco-2 cells, cellular uptake of studied liposomes was evaluated and chitosan-coated liposomes were revealed as the carriers that enable the highest cellular accumulation level in comparison to the non-liposome formulation and uncoated liposomes. In later work<sup>63</sup> a similar approach for improving bioavailability was undertaken, however, as the coating material, the polymer Eudragit L100 was applied. For ensuring the highest encapsulation efficiency of ALN (49.39%) the optimal lipids molar ratio was found as 4:3:1 for phosphatidylcholine (PC): cholesterol (Ch): lecithin (Lec). The authors tested the liposomes composition modification with positively and negatively charged lipids, stearylamine (SA) and dicetyl phosphate (DP), respectively. They found that liposomes with DP exhibit the lowest percentage of released alendronate during the first 2 hours at pH=1.2 and thus for further studies, PC:CH:Lec:DP 4:3:1:1 nanoparticles coated with EuC was selected. Finally it was revealed that carriers of optimized composition allowed for a 12-fold increase in ALN bioavailability compared to pure drug.

## Nanotubes

One of the most widespread inorganic-based nanocarriers are carbon or titanium nanotubes. They not only have tractable properties but additionally possess a synergetic therapeutic effect.<sup>44</sup> The drug release from nanotubes is based on diffusion rates, which vary with drug size and charge, with a dimension of nanotubes, its interactions with a carrier molecule, dimensions, as well as the surface chemistry. Therefore, various strategies can be applied to facilitate the appropriate diffusion of drugs from nanotubes.<sup>64</sup> TiO<sub>2</sub> nanotubes (TNT's) might be created at the surface of titanium implants by electrochemical anodization, which increases the implant area and wettability. Additionally, coating implants with nanotubes allow for improved antibacterial properties and the possibility of implementation of different drugs and proteins. Moreover, their low cost and simplicity in manufacturing are also of great importance, especially considering the potential application. TNT's can provide multi-drug release due to their high loading capacity, high surface area, tunable dimensions, and geometries.<sup>64</sup> Titanium-based implant with antiresorptive properties was proposed by Shen et al<sup>65</sup> by the implementation of alendronate-loaded hydroxyapatite-TiO<sub>2</sub> nanotubes (TNT-HAp-ALN). Structures were prepared sequentially by: anodic oxidation, HAp deposition, and drug loading. The examination of the wettability of the final product revealed its super hydrophilic properties. By comparing the release of alendronate from TNT and TNT-HAp, it was clearly demonstrated that the addition of the hydroxyapatite not only increased the amount of loaded drug, but also significantly prolonged its release – up to 504 hours for modified TNT. However, when the pH of the medium was lower (about 4.5), all of the incorporated ALN was released during 12 hours. The developed system exhibits also notable higher osteoblast proliferation compared to TNT and TNT-HAp, which was confirmed by CCK-8 assay, ALP activity, mineralization, and gene expression evaluation. Further biological studies revealed superior anti-osteoclast capacity of the TNT-HAp-ALN. Finally in vivo experiments performed on the osteoporosis rabbit model followed by micro-CT analysis, X-ray observation, and hematoxylin and eosin (H&E) staining demonstrated that after 3 months from implantation the new bone with a compact structure and the highest interfacial strength was formed around the TNT-HAp-ALN system (see Figure 6).

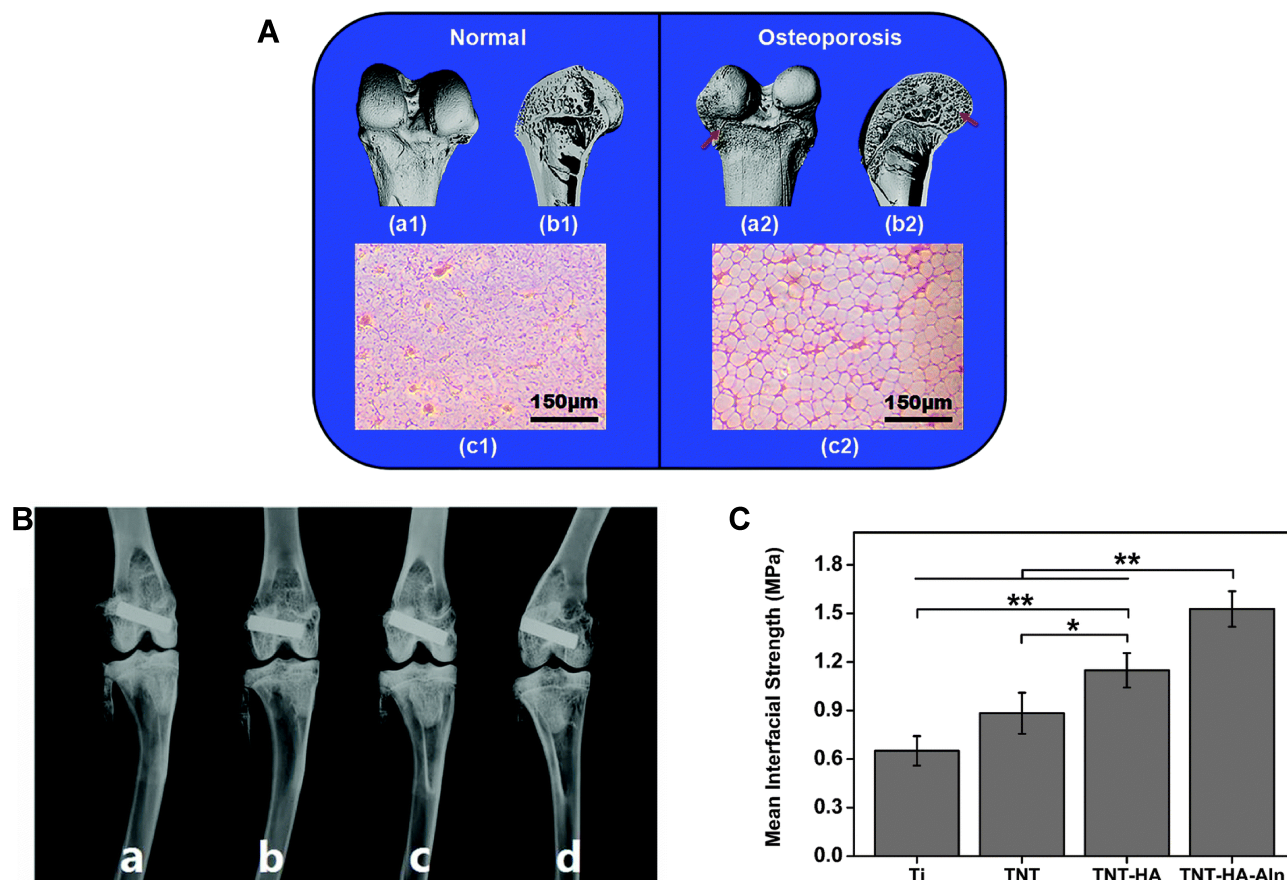


**Figure 6** (A) Micro-CT (a1, b1, a2, b2) and H&E staining (c1, c2) assays for normal (a1–c1) and osteoporotic (a2–c2) bone after implantation for 3 months; (B) X-ray photographs of Ti (a), TNT (b), TNT-HA (c), and TNT-HA-Aln (d) after implantation for 3 months; (C) push-out strength of different implants after implantation for 3 months (n = 4), \*p < 0.05 and \*\*p < 0.01.

**Note:** Used with permission of Royal Society of Chemistry, from Shen X, Ma P, Hu Y, et al. Alendronate-loaded hydroxyapatite-TiO<sub>2</sub> nanotubes for improved bone formation in osteoporotic rabbits. *J Mater Chem B*. 2016;4(8):1423–1436. Copyright 2016; permission conveyed through Copyright Clearance Center, Inc.<sup>65</sup>

Carbon nanotubes (CNTs) have a wide application due to their ultralight weight, thermal, chemical, mechanical, and electrical properties, high aspect ratio, and nano-sized needle structure. A distinctive hollow morphology, which contains sheets of graphene, can be multi-walled or single-walled – based on the number of graphene sheets that are rolled together at specific angles. When nanotubes are functionalized, they are soluble in water and the long circulation in the serum can be achieved. Carbon nanotubes are used as drug delivery vehicles, artificial implants in tissue engineering, as well as peptide and gene delivery.<sup>44</sup> An innovative drug carrier in the form of multi-walled carbon nanotubes (MWCNTs) has been proposed as a potential ALN delivery system.<sup>66</sup> Alendronate, neridronate, and pamidronate as three classes of bisphosphonates were conjugated onto MWCNTs. Before the conjugation, the MWCNTs were first oxidized which provided carbon nanotubes with carboxylic acids which can be further functionalized for biological moieties' adhesion. Importantly it also renders the MWCNTs hydrophilic, therefore less cytotoxic. Subsequently, oxidised MWCNTs were reacted with thionyl chloride to further transform them to acyl chloride entities. Finally, BPs were grafted onto MWCNTs via acyl chloride moieties. Successful conjugation was confirmed employing complementary techniques (SEM, TEM, EDX, FTIR, Raman and TGA). Since the BPs conjugated onto MWCNTs have higher molecular weight, diffusion of the free BPs into the circulating blood is hampered and thus prevents BPs from renal clearance. Nikfar and Shariatinia<sup>67</sup> evaluated the ability of (4,4)-armchair CNT and its three phosphate functionalized forms (CNT-nH<sub>2</sub>PO<sub>4</sub>, n=1–3) as novel DDSs for the two anti-osteoporosis drugs, namely alendronate and etidronate (ET). The authors focused on the application of the density functional theory (DFT) calculations to achieve both the diverse properties and to select the most favorable drug delivery system. It was revealed that the CNT-3H<sub>2</sub>PO<sub>4</sub> system displayed the smallest band gap

energy, chemical potential, and hardness, simultaneously possessing the greatest electronegativity and electrophilicity index. The found values of these parameters provided conditions suitable and effective for the attachment of drugs onto the bone surface, thus inhibiting osteoporosis. Thus, the CNT-3H<sub>2</sub>PO<sub>4</sub> was established as the most appropriate vehicle for both drugs. The authors also evaluated the attachment of pure ALN, pure ET, the ALN-CNT-3 H<sub>2</sub>PO<sub>4</sub>, and ET-CNT-3 H<sub>2</sub>PO<sub>4</sub> drug-carrier systems to the bone tissue. The optimization of mentioned structures bonded to the hydroxyapatite with 17 water molecules (HA)-17 water (w) was modeled. The conclusion was that, among all developed systems, the ALN-CNT-3H<sub>2</sub>PO<sub>4</sub> is the most promising for the osteoporosis treatment. However, experimental studies are still required to assess the potential use of the proposed materials as DDS.

## Gold/Nanodiamonds/Hydroxyapatite (HAp)-Based Systems

Apart from polymeric nanoparticles, gold nanoparticles (GNPs) conjugated with alendronate were tested for inhibition of bone resorption.<sup>68</sup> These structures alone can inhibit RANKL formation and therefore limit osteoclastogenesis while alendronate-loaded could further increase their capabilities for osteoporosis treatment. TGA measurements have shown that 7.32 wt% of alendronate was successfully conjugated to GNPs. After ALN coupling the mean size of uniform nanoparticles did not change significantly (34.7 nm and 32.9 nm for GNPs and GNPS-ALN, respectively). The superior inhibitory effect on osteoclastogenic gene expression was revealed for GNPs-ALN compared with GNPs and ALN alone. Moreover, *in vivo* tests performed on the ovariectomy (OVX)-induced osteoporotic mouse model indicated that the mice treated GNPs-ALN had higher bone density as compared to the control groups. Thus, it has been shown that the developed system can serve as a preventing and treating osteoporosis agent. Ryu et al.<sup>69</sup> considered the use of nanodiamonds (NDs) for alendronate delivery. These sp<sup>3</sup> carbon-based structures could occur in the ultra-nanocrystalline form up to 10 nm. The main advantage is associated with their superior biocompatibility, large area, and high adsorption capacity which could be used for drug coupling.<sup>70</sup> Conjugation of alendronate was conducted by carbodiimide chemistry. Obtained nanostructures exhibit narrow size distribution below 100 nm and a negative charge close to -40 mV. The optimal concentration of alendronate was determined based on cell toxicity *in vitro* tests. The maximum value of ALN, which simultaneously increases the activity of ALP and does not cause cell toxicity, was 0.1 mg/mL. It should be noted, however, that taking into account the affinity to the HAp, the presented conjugates, due to their larger size, were characterized by a lower binding ratio compared to alendronate – 36.73% and 77.50%, respectively. Yet this value was higher than NDs alone, which confirms favorable binding affinity. Importantly, developed nanostructures exhibit significantly higher cellular uptake by MC3T3-E1 cells after 12 h of incubation compared to pure alendronate, NDs, and PLGA-ALD conjugates. Additionally, *ex vivo* fluorescence images revealed that, although pure NDs could accumulate in abdominal organs, NDs-ALN deposition in the bone is more efficient.

Nano-hydroxyapatite (nHA), which is the main component of the mineral fraction of dental tissues and bones, found applications in drug delivery systems fabrication.<sup>71</sup> Porous nHA can be easily loaded with drugs and then used as a targeted delivery system to the bones. Bisphosphonates are well-known for their high affinity to HAp. It was found that deprotonated negatively charged oxygen atoms of the phosphate groups of the BPs interact electrostatically with Ca<sup>2+</sup> cations of HAp.<sup>72</sup> Bosco et al.<sup>73</sup> developed the bone-like hydroxyapatite nanocrystals (nHA) functionalized with alendronate (nHA<sub>ALD</sub>). nHA of the nanoscale sizes below 100 nm and with a high specific surface area (SSA) of 160 m<sup>2</sup>/g was synthesized. The authors confirmed the drug presence on the crystals by means of FT-IR and TGA analysis and postulated that all ALN adsorbed on nHA was chemically linked while the amounts of physisorbed drug were insignificant. To verify the therapeutic capacity of resulting systems *in vitro* osteoclastogenesis tests on RAW264.7 cell line were performed. It was revealed that nHA with ALN attached considerably reduced the number of osteoclast-like cells. Using the electrospray deposition (ESD) method, the potential of the developed materials for the fabrication of bone implant coatings for application in osteoporotic patients was also demonstrated. HAp-based nanoparticles for alendronate delivery were also proposed by Hwang et al.<sup>74</sup> Pure HAp nanocarriers were beforehand coated, employing a layer-by-layer (LBL) technique with three layers of poly(allylamine) (PAA) and alginate (ALG). Obtained ALN-LBL-HAp nanoparticles had zeta potential equal to -21.1±4.2 mV and their size was below 100 nm. The addition of ALN into NPs improved absorption on TCP disk from 26% for pure LBL-HAp nanoparticles to 80%. Biological experiments *in vitro* demonstrated that prepared structures significantly increased the number of MC3T3-E1 cells, while the proliferation

of RAW264.7 cells was only slightly enhanced during 7 days of culturing. Additionally, considerably greater ALP activity exhibited cells that were cultured on the developed materials compared to pure HAp, LBL-HAp, and the control group.

## Microspheres/Microparticles as DDS

Microspheres/microparticles could also be used as drug delivery systems with distinct advantages in comparison to traditional forms. These formulations enable to avoid the first-pass metabolism, reduce gastrointestinal irritation, as well as allow for prolonged drug release.<sup>75</sup> Microparticles protect the transported substance from undesirable degradation and have the ability to be injected directly into the targeted tissue.<sup>76</sup>

Microspheres (MP) for ALN delivery were fabricated in the form of nanocrystalline hydroxyapatite biomimetically mineralized and deposited on aminated modified polylactic acid (EPLA).<sup>77</sup> Successful deposition and ALN loading were confirmed by SEM, XRD, and FTIR analysis. The authors demonstrated that the amount of loaded drug into EPLA-nHAp microspheres was strictly related to the initial concentration of ALN up to 17 mg/mL. Additionally the equilibrium of adsorption time was estimated as 20 h, which led to the adsorption capacity of EPLA/nHAp equal to 2.46 g/g when 94% HAp content was selected. The applied methodology of nHAp deposition on EPLA microspheres allowed for obtaining a larger pore volume and specific area compared to pure EPLA microspheres. Furthermore, this modification provided a more sustained release of alendronate (56% during 15 days). In vitro tests confirmed the biocompatibility of prepared microspheres which ensured favorable cell adhesion and proliferation. Yang et al<sup>78</sup> obtained hollow hydroxyapatite microspheres, composed of two hemispheres loaded with alendronate. The loading capability of synthesized structures was revealed to be 46.8wt%. During the first 2 days, only 7% of ALN was released which was explained based on the high alendronate affinity to HAp and the hollow and porous structure of the carrier. After 72 hours of incubation, 2 µg/mL HAp-ALN showed a superior ability to promote MSCs proliferation. However, it was observed that HAp-ALN caused cell aggregation. In vitro tests on mBMSCs cells demonstrated that HAp-ALN moderately inhibited expression of ALN in osteoblasts and enhanced expression of RUNx2, OC and Col to a greater extent compared with pristine HAp microspheres. As with nanoparticles, PLGA is also the preferred choice for microparticle (MP) fabrication. Research presented by Bae and Park<sup>79</sup> focused on the preparation of injectable systems for alendronate delivery. The authors formulated PLGA microspheres by multiple emulsion technique with hyaluronic acid (HA) in the inner aqueous phase and co-solvent in the organic phase. Conventional PLGA microspheres exhibited low encapsulation efficiency of about 1%, which was herein overcome by modifications of MP composition. The mean particle size of all prepared systems was in the range of 20–70 µm. When particles with HA were prepared with dichloromethane and acetone, the encapsulation efficiency increased to 73.52%. Additionally, acetone allowed for prolonged release and limited initial burst – alendronate was detectable for more than 4 weeks after administration in rabbits. The maximum plasma concentration of alendronate reached 82.9 ng/mL on day 7. High- and medium-dose alendronate microspheres showed superior trabecular bone areas after 2 months of treatment – 482% and 394%, respectively, compared to the control group. Additionally, these systems caused the tighter, denser, and stiffer structure of the proximal tibia and increased the formation of cortical and cancellous bone mass compared to control and underwent placebo surgery groups. Microspheres composed of triblock copolymer poly(L-lactide)-poly(ethylene glycol)-poly(L-lactide) (PLLA-PEG-PLLA) and obtained by double emulsion method for alendronate delivery were proposed by Wei et al.<sup>80</sup> Additionally, coating with gelatin followed by biomineralization in simulated body fluid (5xSBF) was employed. All of the obtained microspheres possessed 2–8 µm average pore size and ~150 µm average diameter. After 24 h of biomineralization, 28wt% deposition of minerals was achieved. From the initial ALN concentration equal to 25 µM or 50 µM, the loading capacity was 1.4 mg or 2.5 mg per 1 gram of microsphere. It was found that 50% and 60% of the incorporated drug was released during 21 days from structures loaded with lower and higher amounts of ALN, respectively. Further experiments revealed high expression of COL-I and OCN genes, BMP2, and OPN proteins for the later microspheres. The biocompatibility of developed microspheres was confirmed in in vivo tests in rabbits. Additionally, for the system with the highest amount of drug, more pronounced angiogenesis resulting in vascular tissues was detected.

## Mesoporous-Based Structures

In recent years, extensive research has been carried out on mesoporous drug delivery matrices. The high surface area and pore volume of mesoporous structures allow for incorporation of the large amount of transported drug which could be release controlled due to a homogenous and ordered pore network.<sup>81</sup> The most common inorganic component is silica; however, mesoporous carbon could also be implemented for this kind of application. The main advantages of silica-based mesoporous nanoparticles over other types of particles include the robustness of the silica framework, which allows the use of harsh reaction conditions for their modification, and their excellent textural properties. In fact, conventional polymeric nanoparticles usually present low drug capacity, less than 5% of total weight, whereas these silica-based mesoporous nanoparticles offer greater efficiency.<sup>2,82</sup> Except for serving as a drug reservoir, the silica matrix provides a protective shell for the molecules against potential pH- or enzymatic-mediated drug degradation in the organism. The mesoporous silica materials (SMM) were employed as a delivery system for alendronate by Balas et al.<sup>83</sup> For this purpose two types of hexagonal SMM, MCM41 (DP=3.8 nm) and SBA-15 (DP=9.0 nm) materials were selected for the loading and controlled release of alendronate. As expected, it was found that the highest surface areas of SMM promoted the greatest amounts of loaded drug. Moreover, ALN loading increased when SMMs were organically modified with aminopropyl groups. This modification allowed for an almost three-fold increase of loaded ALN which achieve 22%, 37%, 8%, and 14% for SBA-15-NH<sub>2</sub>, MCM41-NH<sub>2</sub>, SBA-15, and MCM41, respectively. This was attributed to the strong interactions between the phosphonate groups in ALN and the amino groups covering the silica surface. Colilla et al.<sup>84</sup> proposed another modification of SBA-15 mesoporous silica matrices with phosphorous groups to increase interaction between matrix and alendronate. Modification with P<sub>2</sub>O<sub>5</sub> changed the 2D-hexagonal structure of P-SBA-15 to rectangular in a higher amount of phosphorus groups, decreased the textural properties of samples compared to pure SBA-15, and increased the wall thickness. After 24 h soaking in ALN solution, matrices with P<sub>2</sub>O<sub>5</sub> loaded a two times higher amount of this drug compared to pure silica.

An interesting bioinspired approach for the fabrication of mesoporous biosilica-based nanostructured material for the treatment of bone disease was presented by Cicco et al.<sup>85</sup> ALN was in vivo incorporated into biosilica shells of cultured *Thalassiosira weissflogii* diatoms, by feeding the algae with an aqueous solution of the drug. Subsequently, ALN-functionalized mesoporous biosilica were recovered from diatoms with the removal of organic matter and tested as osteoinductive support. The successful incorporation of the drug was proven by FTIR, EDX, <sup>1</sup>H, <sup>13</sup>C, and <sup>21</sup>P NMR analyses. Additionally, increased hydrophilicity of resulting ALN-biosilica, compared to pure biosilica, was also used as an indicator of alendronate incorporation. The biocompatibility of developed materials was demonstrated in vitro with the use of SaOS-2 osteosarcoma cells and BMSC. Furthermore, the authors examined the therapeutic effect of obtained ALE-biosilica systems and revealed the strong inhibition of osteoclast-like cells (J774 cell line) metabolism. It was found that estimated as 1.45% w/w via TGA the loading percentage of ALN was able to reduce the metabolic activity of J774 cells by 5% compared to the glass control (see Figure 7).

Saha et al.<sup>86</sup> tested various mesoporous structures based on carbon and doped with nitrogen for alendronate delivery. The estimated BET surface for these materials was 1.066 m<sup>2</sup>/g, while the pore size distribution was not uniform, since narrow regions of micropores (0.35; 0.5; 0.785 nm) and mesopores (2–9 nm) were present. The total pore volume was equal to 0.6 cm<sup>3</sup>/g and the total loading of alendronate was 5%. Mediums at different pH were utilized for studying alendronate release. Pure alendronate was completely dissolved during 30 minutes at pH=1.2. For comparison, when mesoporous carbon was incubated at pH=1.2 only 20% of the total amount of alendronate was released, whereas 64% of ALN was released in the medium at pH=7.4. These differences were explained by the weaker hydrogen bonds between ALN and nitrogen in a more alkaline environment. Moreover, doping with nitrogen allowed the adsorption of more than twice the amount of alendronate compared to unmodified structures. Also, the mesoporous bioactive glass-based microspheres (MBG-MSs) were studied as bisphosphonate carriers due to their homogeneity, large pore volume, and surface area.<sup>87</sup> Developed systems were prepared by emulsification and evaporation-induced self-assembly. Doping the glass with CaO allowed for the higher formation of calcium phosphate apatite phase after 24 h soaking in SBF. Prepared structures with CaO had complex pore size distributions – around 2.9 nm, 4.75 nm, and 15 nm. High ALN loading in the range 641–776 mg/g for all tested MGB-MSs was observed. Cell viability and proliferation activity assay revealed that,

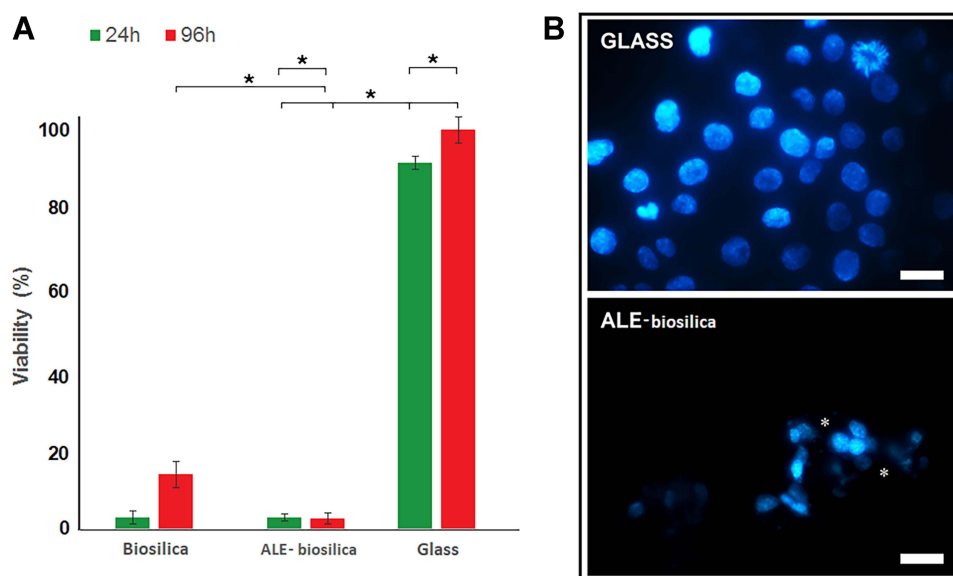


**Figure 7 (A)** The percent viability of J774 cells incubated on biosilica, ALE-biosilica, and on glass as the control. Differences (\*) were considered statistically significant for  $p < 0.05$ ; **(B)** DAPI staining of J774 cells grown on glass and ALE-biosilica after 96 h showing nuclei fragmentation and apoptosis (\*). Marker: 25  $\mu\text{m}$ .

**Note:** Reprinted from Cicco SR, Vona D, Leone G, et al. In vivo functionalization of diatom biosilica with sodium alendronate as osteoactive material. *Mater Sci Eng C*. 2019;104:109897. Copyright (2019) with permission from Elsevier.<sup>85</sup>

although no significant growth of rBMSCc cells was observed during the first 7 days of culture, the presence of CaO and  $\text{P}_2\text{O}_5$  in microspheres allowed for an increase in proliferation of studied cells after 14 days of the biological experiment. It was concluded that prepared MGB-MSs systems after doping with CaO could serve as the efficient and bioactive ALN carriers.

## Metal-Organic Framework (MOF)-Based Systems

Metal-organic frameworks (MOF), a kind of organic-inorganic hybrid porous materials composed of metal ions and organic linkers have drawn increasing attention and became promising structures in various biomedical fields. Due to unique properties, such as large pore volume, high surface area, good biocompatibility, water solubility, biodegradability and high drug loading efficiency, MOFs have also found applications as drug delivery systems.<sup>88</sup> Importantly, drugs/biomolecules can be incorporated into MOFs in a variety of ways, including pore encapsulation, surface adhesion, covalent linkage, and forming bio-MOF (metal-biomolecule frameworks), which makes them an excellent DDS with great encapsulation features.<sup>89</sup>

Vasaki et al<sup>90</sup> exploited the potential of phosphonate MOFs as a delivery platform for anti-osteoporosis medications. Designed systems were composed of biologically acceptable  $\text{Ca}^{2+}$  and  $\text{Mg}^{2+}$  ions and selected bisphosphonate drugs (including ALN, etidronate, pamidronate, and neridronate) as the organic ligands. The authors assessed the kinetic release of the drugs under conditions mimicking those of the human stomach ( $\text{pH}=1.3$ ) as the materials were obtained in the form of tablets. As a control samples the tablets containing free BPs were tested. For all studied samples the coordination of BPs drug to  $\text{Ca}^{2+}$  significantly decreases the release rate and percent of the final release. In the case of Ca-ALN based systems the initial release rate was substantially hampered compared to control from 0.75  $\mu\text{mol}/\text{min}$  to 0.26  $\mu\text{mol}/\text{min}$ , respectively. The final % release was reduced almost two times. The replacement of  $\text{Ca}^{2+}$  ions with  $\text{Mg}^{2+}$  in the ALN system causes a structural transformation and considerably influenced the release characteristics. The calculated initial released was equal to 0.08  $\mu\text{mol}/\text{min}$ , whereas the final release after 192 h reached the value of only 8%. The authors assumed that the observed slowdown in drug release is a consequence of the M-O phosphonate coordination bond resistant to acid-induced hydrolysis of BP ligand. The preliminary biological

tests on NIH3T3 embryonic cell lines have not revealed the significant differences in cell viability when comparing to control samples.

Recently Al-Baadani et al<sup>91</sup> presented a novel multifunctional MOF-based system for ALN delivery. Electrospun polycaprolactone/gelatin (PG)-blended membrane was embedded with ALN-loaded zeolitic imidazolate framework-8 (ALN/Zif-8) nanoparticles employing solution-phase synthesis. Zif-8, a typical Zn-based MOF, was applied for its ability to improve osteoblast function and simultaneous bacterial growth hampering.<sup>92</sup> The authors performed the physico-chemical characterization of designed systems and confirmed the successful synthesis of PG/Aln-Zif-8 nanofibers with excellent mechanical characteristics. The release studies carried out in PBS buffer (pH=7.4) revealed the synergistic effects of the coordination bonds among ALN, zinc ions, and organic ligands on the regulation of drug and Zn<sup>2+</sup> release. The release profile obtained in the PG/ALN-Zif-8 group showed that Zif-8 nanoparticles significantly reduced the burst release of ALN by approximately 75% compared to the control group. The authors postulated that encapsulated drug is at first released through the dissolution of the drug-Zif-8 coordination bonds, rather than through the diffusion process. The antiosteoporosis and osteoinductive properties of developed PG/Aln-Zif-8 membranes were demonstrated in *in vitro* studies on MC3T3-E1 and RAW264.3 cells. The antibacterial activity of obtained materials against both *Staphylococcus aureus* and *Escherichia coli* was also confirmed. Finally, *in vitro* evaluation on osteoporotic rats demonstrated that designed systems efficiently promote osteogenesis. Presenting multifunctionality of obtained MOF-based membranes make them promising systems for clinical application in bone tissue engineering.

## Calcium Phosphate Ceramics/Bone Cements-Based DDS

Since the calcium orthophosphates represent the main inorganic component in bone tissue, the use of synthetic forms of this group of compounds appears appropriate for bone regeneration, including also ALN delivery systems.<sup>93,94</sup> Synthetic hydroxyapatite exhibits the most similarities to the calcium phosphates in the mineral part of the bone, however other types such as octacalcium phosphate (OCP) and tricalcium phosphate (TCP) are also employed in this field.<sup>95</sup> To incorporate bisphosphonates into calcium phosphate, and therefore increase the biological performance of this structure, two methods are the most commonly utilized, namely the co-precipitation in an aqueous medium and the chemisorption from solution. Forte et al<sup>96</sup> presented research regarding the synthesis and characterization of OCP as a carrier of alendronate and zoledronate. The highest concentration of ALN that allows for the OCP formation was equal to 1.2 mM and the highest amount of this drug incorporated in the solid product was 5.2wt%. Based on the release profiles the authors concluded that part of the drug was loosely bound to OCP, which could be the reason for the initial burst release. Pure OCP in water hydrolyzes to HAp, however, when ALN was incorporated into the structure, the conversion to HAp was not observed even after 30 days. Therefore, it was postulated that alendronate increased the stability of OCP structure but enhanced thermal stability was not detected. *In vitro* studies revealed that developed OCP-ALN systems caused a decrease in both osteoclast viability and differentiation. Other studies regarding the application of calcium phosphate bone cement as bisphosphonates carriers were presented by Panzavolta et al.<sup>93,97</sup> Whereas Dolci et al<sup>98</sup> developed a bisphosphate-based hybrid system for alendronate delivery. The authors focused on the implementation of ALN-loaded microparticles into calcium phosphate cement (CPC). In the first step, the solid lipid microparticles were prepared by the environmentally friendly spray congealing method. Indirect incorporation of ALN into the cement by the means of SLM was expected to decrease the alendronate release and therefore allow for cement's setting. Four different substances were selected for microparticles fabrication: stearic acid, Precirol ATO5 (Pre), stearyl alcohol, cutina HR (Cut), and Tristearin. The size of the obtained structures was in the range of 100–150 microns, and the loading of the alendronate 10%w/w did not influence the spherical shape and dimension of MP. As expected a high encapsulation efficiency (>90%) was obtained. The conversion of  $\alpha$ -TCP to poor crystalline hydroxyapatite in soaked CPC was prolonged to 21 days when MP-ALN was applied in comparison to pristine MP, in which the conversion was finished after 7 days of soaking. Additionally, no apparent change in mechanical properties was triggered by the presence of ALN-MP in the CPC-Cut-ALN and CPC-Pre-ALN (systems based on calcium phosphate cement and cutina or precirol, respectively) even after 21 days of soaking in PBS. Moreover, the controlled release was achieved for all tested systems – more than 90% of alendronate was released during the first 4 hours, however, the time release from tristearin MPs was longer. Overall the CPC-Cut-ALN and CPC-Pre-ALN were found to be the most promising systems for alendronate

delivery. Calcium phosphate cement–PLGA composites were also proposed as ALN delivery systems.<sup>99</sup> In another work biphasic calcium phosphate (BCP) in the form of scaffolds loaded with alendronate was developed for bone regeneration.<sup>100</sup> Authors prepared two systems with various amounts of alendronate, namely ALN (1 mg)/BCP and ALN (5 mg)/BCP, for which the loading efficiency (LE) was 78.63%, and 72.77%, respectively. More than 70% and less than 20% of drug loaded in ALN (1 mg)/BCP and ALN (5 mg)/BCP were released for 28 days. Biological tests *in vitro*, including evaluation of ALP activity, osteopontin, and osteocalcin expression, demonstrated superior properties of scaffolds with a higher amount of drug. Importantly, employing the rat tibial defect model, the authors observed that after 4 and 8 weeks of an experiment, ALN (5 mg)/BCP scaffold provided increased bone formation volume compared to the control group with abundant osteoid tissue.

## Coatings as a Procedure for DDS Fabrication

Implants for bone fixation that are prepared from biodegradable polymers such as PLGA, PLA, or PGA do not promote bone rebuilding or reduction of bone loss, therefore they do not prevent future fractures. In addition, progressing fractures can also destabilize implants and may result in the need for another surgery.<sup>101</sup> Due to the low bone density and therefore delayed bone healing in osteoporotic patients, loosening of the fixation system could occur more frequently. Therefore, it seems necessary to deliver both drugs limiting bone resorption and implants at the same time.<sup>102</sup> In this aspect, Hur et al<sup>103</sup> proposed the coating of bioabsorbable bone already in clinical use with a blend of ALN and azidobenzoic acid-modified chitosan photo-crosslinked by UV irradiation (AL-Az-CH\_P). The coated surface was rough and wrinkled in comparison to pristine smooth plates, and stable up to 120 days in PBS. When lysozyme was applied, gradual degradation was observed. The high loading efficiency of alendronate was achieved – more than 97% of the theoretical amount of drug per plate was incorporated. Additionally, in a medium with and without lysozyme, the sustained release was observed for 63 days maintaining thus a therapeutically effective drug level. When cytotoxicity experiments were performed after 7 days of culture, the number of MG-63 cells increased significantly for (AL-Az-CH\_P) in comparison to the control plates. Importantly the authors tested developed materials *in vivo* regarding their ability for bone regeneration. After 8 weeks of implantation, the micro-CT evaluation revealed that the group with the ALN-loaded plate exhibited a significantly higher volume of newly formed bone (about 53%) than the groups without the drug (14–24%). Moreover the satisfactory *in vivo* biocompatibility of the obtained system was also demonstrated. Thus, an interesting system for both bone fixation and its accelerated repair was presented. Boanini et al<sup>104</sup> studied calcium alendronate and octacalcium phosphate coatings deposited on titanium substrates by matrix-assisted pulsed laser evaporation. Successful incorporation of calcium alendronate into thin films and their deposition on titanium substrates was achieved. Osteoblasts cultured on prepared systems showed good viability even when alendronate was the only component of the coating. However, when considering osteoclastogenesis, the presence of alendronate seems to be crucial for its inhibition. It was found that the viability and proliferation of osteoclasts were significantly lower when ALN was applied and these alterations were caused by the downregulation of RANKL. Another work utilizing titanium substrate as a platform for ALN delivery was presented by Zheng et al.<sup>105</sup> The authors immobilized alendronate onto Ti (by incubation in ALN solution of various drug concentrations) which was previously modified utilizing two various approaches: i) plasma treating and ii) APTES and glutaraldehyde coating. A significantly higher amount of ALN was anchored in the second method. A similar alendronate immobilization was achieved only when four times more of the drug was introduced to the plasma treating-titanium substrate. Additionally, the total amount of ALN released during the first 14 days constitutes less than 10% for Ti modified with APTES which was significantly lower than for plasma treated titanium – 33% and 40% for applied initial alendronate solution of 2.5 mg/mL and 1 mg/mL correspondingly. However, ALP activity profiles for osteoblasts revealed no significant differences between the type of immobilization and osteoblast differentiation during the first 10 days. Additionally, the presence of alendronate allowed for a significant increase in ALP activity on day 7 compared to pristine titanium when hMSCs were considered. Finally, the highest expression of RUNX2, OXS, OPN, and OC markers was observed in hMSCs cultured on the APTES-treated titanium substrate with alendronate immobilized.

Self-assembly capabilities of alendronate on the oxide surfaces were utilized by Bronze-Uhle et al<sup>106</sup> to form a coating on the UV-treated titanium surface covered thus with hydroxylated TiO<sub>2</sub> layer. Immobilization of ALN

performed on the oxidized titanium surface allowed for both the increase of the free energy and hydrophilicity which was manifested by contact angle decrease. Biological testing showed an increase in viability of MC353-E1 pre-osteoblast cells for functionalized with alendronate surfaces after 24 h of culture, however, these changes were not as significantly pronounced after 48 h of culture. In vitro tests have not revealed any mineralization in the developed substrate after 14 days of the experiment, even though higher cell adhesion was observed. Hydroxyapatite coating is commonly utilized for titanium substrates for the promotion of tissue growth, osteoconductivity, and bonding to the bone. For further enhancement of this biological coating, Bose et al<sup>27</sup> proposed the application of magnesium-doped hydroxyapatite coatings with incorporated alendronate and additional coating made of polycaprolactone (PCL) for the facilitation of controlled drug release. It was demonstrated that without PCL coating, 75wt% of ALN was released during the first 12 hours, however, 2wt% and 4wt% of PCL coating decreased the initial burst release of the drug to 34% and 26%, respectively.

## Polymer Conjugates/Composites

Significant advantages over traditional drug formations are offered by polymer–drug conjugates. Improved solubility of medicine in these types of formulations leads to enhanced bioavailability. Furthermore, the controlled delivery could be achieved by the introduction of targeting moieties, which in turn limit side-effects associated with the fluctuations of the active substances concentrations.<sup>107</sup> Importantly, the conjugation of drugs to polymer could improve its pharmacokinetics and pharmacodynamic.<sup>108</sup> Pan et al<sup>109</sup> fabricated systems in which alendronate and D-aspartic acid octapeptide were conjugated to N-(2-hydroxypropyl)-methacrylamide (HPMA) copolymer. Retention of the prepared conjugates was strongly correlated with their effective diameter and was the longest (about 72% of the original dose after 48 h of implementation) for the system with the higher amount of ALN conjugated to the polymer of high molecular weight (C-Hh). It was found that all obtained structures accessed the bone after 15 minutes of injection, whereas a half-time of terminal elimination was longer for large molecular-size structures. Interestingly, when comparing the efficiency of binding of HPMA copolymer, low molecular weight systems with a higher amount of alendronate allowed for larger binding. This correlation was not observed for high molecular weight conjugates since in this case, ALN content did not significantly influence binding efficiency. Additionally, the deposition of C-Hh on HAp was lower in comparison to conjugate with smaller alendronate content. A different approach was presented by Xie et al.<sup>110</sup> They synthesized conjugates with alendronate and EP4 agonists responsible for the suppression of apoptosis of osteoblasts cells. The authors expected that these two compounds could have a synergistic or additive effect on bone formation. As a linker, dipeptide-para-aminobenzyl alcohol (Leu-ARG-PABA) was used. Utilized radiolabeling allowed for the determination of uptake into bones and pharmacokinetics of developed conjugates. In vivo experiments on OVX rats as an animal model revealed that 50% of the EP4 agonist was unable to effectively bind to the bones. Moreover, a half-time of release for alendronate was up to 5 days with 5 µg/kg/day rate. The self-assembling bisphosphonate-based conjugates were proposed by Tang et al.<sup>111</sup> For achieving the locally concentrated delivery of ALN, alendronate-derived hydrogelator N-[(9H-Fluoren-9-ylmethoxy)carbonyl]phenylalanylphenylalanine [(Fmoc-Phe-Phe-alendronate(Aln-D))] was synthesized. The stability of obtained systems at room temperature was confirmed for up to 1 month. Prepared samples showed superior inhibitory properties for BMMS cells compared to pure alendronate, especially when considering lower concentrations of the drug. In addition, developed materials did not inhibit the osteoblasts proliferation up to 96 h. It was also demonstrated that a lower concentration ALN-D was required for osteoclast apoptosis compared to plain ALN. Additionally, in vivo tests revealed that 0.39 µM ALN-D decreased resorption area to 19.8% (compared to the resorption area of the control group).

## Hybrid Materials

### Hydrogels as Delivery Systems

Hydrogels are a type of three-dimensional polymeric network that possess superior swelling and shrinking capabilities. Appropriate porosity and the ability to mimic natural ECM of the bone make them promising materials for application as drug delivery systems. Furthermore, the usage of degradable polymers allows for the fabrication of an absorbable

structure that could eliminate the need for surgical removal after implementation. Moreover, injectable hydrogels that might be manipulated via a relatively non-invasive manner and provide precise filling are of great interest in bone tissue engineering. The benefits of using injectable systems for bone defects, especially those irregularly shaped, include ease of use, shorter surgical times, minimal scarring, and thus overall greater patient comfort.<sup>47,112</sup> The main problem associated with hydrogels is their incompatibility with hydrophobic drugs that, however, could be overcome with modification of hydrogel structure by changing their crosslinking degree or/and method of preparation.<sup>113–115</sup> In addition, due to intrinsic permeability and limited network interactions with small molecule drugs within the hydrogel matrix, sustained delivery using such macromolecular systems remains a challenge. Therefore, to enhance the therapeutic effect and provide localized application and support for the defects the nano/microformulations are increasingly combined with hydrogels to fabricate hybrid systems for controlled drug delivery.

Injectable hydrogels with alendronate-loaded PLGA nanoparticles were proposed by Posadowska et al.<sup>116</sup> Double emulsification/solvent evaporation technique (DES-E) was employed for the preparation of PLGA-ALN nanoparticles which resulted in a similar hydrodynamic diameter (234 nm) and higher encapsulation efficiency (70.3%) compared to the previously mentioned work by Cohen-Sela et al.<sup>54</sup> when DES-E was also applied. Crosslinking of gellan gum-based hydrogels was performed with calcium ions and PLGA-ALN nanoparticles were suspended in the prepared matrix. The addition of NPs-PLGA-ALN lowered the swelling of hydrogels, however, their injectability and extrusion force were not affected by this modification. Moreover, rheological tests revealed that prepared systems were not only elastic but also had the capability to self-heal after damage. Importantly, hydrogels released only 8% of incorporated alendronate after 25 days. By comparison, at this time release from nanoparticles was already finished, which suggests that the prepared systems were appropriate for prolonged alendronate delivery. Biological experiments *in vitro* revealed that no changes in MG-63 cells occurred after culture with hydrogels. Additionally, therapeutic features of developed systems were demonstrated since RANKL stimulated RAW 264.7 cells did not undergo osteoclastic differentiation. Biodegradable and thermosensitive chitosan (CS)-based hydrogel loaded with alendronate was presented as an injectable formulation for osteoporosis treatment.<sup>23</sup> Application of  $\beta$ -glycerol phosphate disodium salt pentahydrate ( $\beta$ GP) as a crosslinking agent delivered thermoreversible properties and allowed for superior degradation and swelling. It was found that optimized gelation time in the range of 0.5–3 min exhibited a system with chitosan concentration equal to 2% w/v. After the incorporation of alendronate, longer gelation periods, smaller pore size, and more condensed structure were observed. Stability tests revealed that, prior to storage, prepared systems should be lyophilized. For 2, 5, and 10 mg of alendronate concentration, cumulative drug release reached almost 100% after 30, 45, and 60 days, respectively. In *in vivo* experiments the rapid gel formation within 15 min post-injection in rats and gradual biodegradation of hydrogels after 1, 2, and 3 weeks were observed. Furthermore, for ALN-loaded system, faster maturation of granulation tissue, and faster proliferation with less inflammatory response were obtained in comparison to plain thermogel. Skeletal uptake in rats was more than 50% of ALN initially loaded into hydrogels. Papathanasiou et al.<sup>117</sup> proposed injectable, responsive and programmable smart silica hydrogels for the controlled delivery of selected bisphosphonates including alendronic acid, etidronic acid (ETID), pamidronic acid (PAM), and neridronic acid (NER) among others. Prepared systems did not absorb additional water, and the transition from hydrogel to dry sample was not reversible. During the first 48 h, close to 70% of initial alendronate was released. However, the study showed, that drugs like NER, PAM, and ALN have a similar release trend, and by observing step-wise, sustained release up to 144 h for NER and PAM, we can assume that, after initial plateau, ALN will also undergo similar release. Additionally, the possibility for the re-loading of drug was shown for the ETID.

Utilization of tetra-PEG hydrogels as injectable systems for prolonged ALN delivery was proposed by Li et al.<sup>118</sup> Linear PEG functionalized with alendronate was synthesized with 4-arm-PEG-NH<sub>2</sub> and 4-ARM-PEG-SG, accordingly, and the following dual syringe method allowed for *in situ* formations of tetra-PEG-based systems. The gradual degradation of prepared hydrogels was observed after 28 days in *in vitro* tests. It was found that designed hydrogels exhibit a small initial burst release and subsequently steady release of ALN was observed (up to 28 days), thus indicating effective trapping of the drug within the polymeric network. The cumulative ALN release reached 20% in the first 4 days, which was attributed to free-escaped PEG-ALN prodrugs fracture present on the surface of hydrogels and initial ester degradation of tetra-PEG hydrogels. Biocompatibility of prepared materials was confirmed in *in vitro* culture with

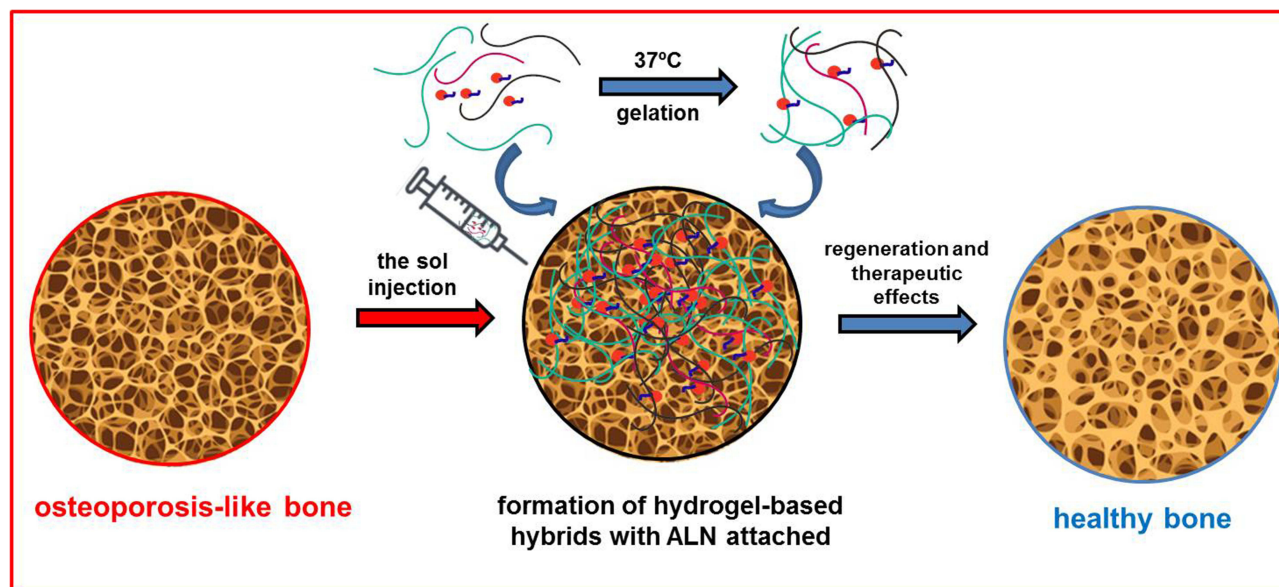


**Figure 8** The schematic illustration of injectable hydrogel-based hybrid ALN delivery systems formation and application.

PDLSCs cells as a model. An *in vivo* experiment in rats revealed some inflammatory response observed 3 days after injection. It was shown that the metabolism of tested systems mainly conducted by the liver and kidney lasted 105 days. DEXA (dual-energy X-ray absorptiometry) and QCT (quantitative computed tomography) methods revealed that BMD was higher in the rats treated with tested hydrogels compared to control groups. Additionally, the strength of bone in the tetra-PEG@PEG-ALN hydrogels was significantly higher and exhibited a greater value of bending pressure after 3 months after materials implementation. Gilarska et al<sup>119</sup> presented a novel hydrogel-based alendronate delivery system for the combined application of osteoporosis treatment and bone regeneration. The multifunctional, biomimetic injectable hybrids that contain ALN molecules coordinated with apatite decorated silica particles, which are immobilized in collagen/chitosan/hyaluronic acid matrix by genipin crosslinking were fabricated. Developed systems provided a non-invasive location of the ALN at the implantation site (by injection), while maintaining the structure, biological properties, and limiting potential adverse effects of the oral therapy. The schematic illustration of injectable hydrogel-based hybrid ALN delivery systems formation and application is depicted in Figure 8. Authors demonstrated that obtained hybrids are efficient osteoconductive materials possessing simultaneously the ability of activation of tissue regeneration model represented *in vitro* by osteoblast-like cells (MG-63) and inhibition of osteoclast-like cells (J7741.A). Furthermore, the biomimetic composition of these materials (biopolymer hydrogel enriched with the mineral phase) allowed for their biointegration (*in vitro* study in SBF model) and delivered the desired physicochemical features. *In vivo* evaluation on a mouse model demonstrated a lack of systemic toxicity of obtained systems as well as their injectability and ability to gel *in vivo*. Importantly it was revealed that developed materials induced angiogenesis. The formation of novel blood vessels was noticed within the hybrids after 60 days of *in vivo* experiment.

## Scaffolds-Based Delivery Systems

Another interesting system for ALN delivery is the multifunctional bone regenerative scaffolds consisting of Poly (L-lactide-co-ε-caprolactone)-based microspheres loaded with bioactive glass-ceramic and alendronate sodium, which was proposed by Mondal et al.<sup>120</sup> The entrapment efficiency of ALN for microspheres loaded using O/W incorporation with 50 mg and 100 mg of the drug was 11.5% and 14%, respectively. For both types of microspheres, ALN-50 and ALN-100, the initial burst was observed and *in vitro* release was detected for up to 50 hours. The system composed of both alendronate and bioactive glass-ceramic and the control sample without drug were evaluated in terms of biological features. The lack of toxicity of both systems was demonstrated with MTT assay for L-929 cells. The promotion of cell adhesion was also confirmed by CLSM evaluation. Kim et al<sup>121</sup> prepared 3D printed alendronate-releasing poly(caprolactone) porous scaffolds by layer-by-layer

technique for enhancing osteogenic differentiation and bone formation in rat tibial defects. Two types of scaffolds with various ALN concentrations were prepared and drug loading of 84.6  $\mu\text{g}/\text{scaffold}$  and 471.6  $\mu\text{g}/\text{scaffold}$  was achieved for the system with 1%wt and 5%wt of alendronate, respectively. The previous studies<sup>122–124</sup> revealed that pristine PCL scaffolds did not cause sufficient enhancement of osteogenic differentiation and proliferation of rADSCs and MG-63 cells. Herein it was demonstrated that MG-63 cells cultured on PCL/ALN systems exhibit higher ALP activity. In vivo study on rat model revealed that 8 weeks after surgery higher bone formation was detected when scaffolds with ALN were employed, which was confirmed by radiographs measurements and micro-CT images. A paper by Ma et al<sup>125</sup> disclosed a two-step process for the preparation of biomimetic hybrid hydrogels as potential tissue engineering scaffolds, containing collagen, hydroxyapatite, and alendronate. The alendronate-coated hydroxyapatite (4.0 wt%) was suspended in genipin cross-linked collagen under physiological conditions. The authors prepared the HAp-ALN system taking advantage of the described in the literature affinity of the drug to hydroxyapatite. Improvement in mechanical properties was observed, as well as an absence of cytotoxic effect against the MG-63 osteoclastic cell line. The work does not disclose any studies that would show a therapeutic effect as well as an improved biointegration. Cattalini et al<sup>126</sup> proposed co-delivery of bioactive agents by utilization of nanocomposite scaffold composed of alginate (Alg) and nano bioactive glass (Nbg). The ionic crosslinking technique with calcium and copper ions was used for the preparation of alendronate-loaded microspheres. Superior encapsulation efficiency (~98.7%) was obtained for alginate–alendronate microspheres. The incorporation of Nbg into AlgCu and AlgCa scaffold did not affect the porosity, however, when both Nbg and ALN were loaded into microspheres, a decrease in porosity was detected. Bioactivity tests using the SBF model showed the formation of hydroxyapatite in all tested systems after 15 days of incubation. When degradation in phosphate buffer (10 mM, pH 7.4) was considered, the systems with  $\text{Cu}^{2+}$  ions showed a higher rate of degradation with respect to systems with  $\text{Ca}^{2+}$  ions after 7 days, which strongly corresponds to the amount of released ions, which was lower for  $\text{Ca}^{2+}$  ions. Higher alendronate release was correspondingly reported for copper-crosslinked systems (89% of the loaded ALN amount), while for calcium-crosslinked systems sustained release in each time frame was revealed and about 56% of ALN-incorporated was released. An increase in ALP activity of rBMSCs (rat bone marrow-derived mesenchymal stem cells) for both systems was observed after 10 days of culture. Additionally, greater proliferation of HUVECs (Human umbilical vein endothelial cells) was recorded and this was attributed to the nontoxic effect of alendronate and angiogenic properties of Nbg. Another approach for the fabrication of hybrid scaffolds for alendronate delivery was presented by Wu et al.<sup>127</sup> Addition of alendronate loaded chitosan/nanohydroxyapatite microspheres (CH/nHA-AL) into poly (L-lactic acid)/nanohydroxyapatite (PLLA/nHA) matrix decreased its porosity from about 89 for the pure systems to 86 and 80 for 10% and 20% CH/nHA-ALN content, respectively. Incorporation of drug-loaded microspheres into scaffolds resulted in slower ALN release for 25 days for tested concentrations compared to controls. However, systems with smaller alendronate content (10%) were characterized by a slower degradation rate. Biological evaluation in vitro on adipose-derived stem cells (ASCs) demonstrated biocompatibility of this system. Moreover after 5 days of culturing increased cells proliferation was revealed compared to scaffolds without microspheres. 3D printed tricalcium phosphate scaffolds coated with polycaprolactone (PCL) for alendronate delivery were studied by Tarafder and Bose.<sup>128</sup> ALN solution in nanopure water was pipetted onto the tricalcium phosphate scaffold. After drying and sterilization, scaffold was subsequently coated with PCL by immersing in 1wt % PCL solution in acetone. Modification with PCL did not affect the compressive strength of prepared scaffolds. Additionally, these systems allowed for more controlled and sustained release of alendronate at pH=5 and pH=7 compared to uncoated scaffolds. The final amount of alendronate in both mediums with different pH was lower compared to systems without PCL and higher for pH=5 for uncoated and coated scaffolds. In vitro tests on hFOB cells confirmed proliferation and cell adhesion on all tested compositions. In vivo tests carried out on male rats revealed that, after 6 weeks from implantation, scaffolds with ALN showed a significant increase in new bone formation compared to systems without the drug. Lower TRAP-positive cells activity for prepared systems indicated inhibition of osteoclast activity. The functionalization of collagen sponge by graphene oxide (GO) for alendronate delivery was proposed by Zeng et al.<sup>129</sup> The addition of GO did not alter the porosity of prepared materials, neither did alendronate influence water uptake and retention. The ALN loading rate was estimated as 45.40 $\pm$ 3.12% and 48.12 $\pm$ 1.99% for Col-0.2%GO-ALN and Col-0.05%GO-ALN sponges, respectively. ALN was released at least for 1 month in the amount of 30  $\mu\text{g}$  from both tested systems. Importantly during the first 4 days, the fast release was observed, next the process was slower in the following test period. Biological experiments in vitro on BMSCs cells revealed that proliferation measured with CCK-8 assay was reduced in the case of Col-0.2%GO-ALN sponges compared to other tested systems. The

highest ALP activity of BMSCs was observed for Col-0.05%GO-ALN sponges which indicated its superior osteogenic features. TRAP-positive osteoclasts were obtained for both mentioned sponges, thus confirming the reduction of osteoclasts proliferation. In vivo tests in osteoporotic rat models demonstrated superior bone resorption when rats were treated with Col-0.05%GO-ALN sponge – new bone volume was  $8.46 \pm 2.44 \text{ mm}^3$  and BV/TV (bone volume over total volume) ratio reached the value of  $47 \pm 12\%$ . It is worth mentioning that in developed systems both alendronate as well as GO promote the formation of new bone tissue.

## The Future Perspectives

Various types of ALN delivery systems have been reported including nano/microformulations, synthetic/natural polymeric and inorganic materials, hydrogel-based materials, scaffolds, coated-like structures, as well as organic–inorganic hybrids. All of them are undoubtedly very interesting from a scientific point of view, however, the complexity of their production/fabrication often limited the possibility of their future clinical application. There are many hydroxyapatite-based alendronate carriers described in the literature. The crucial fact is that ALN exhibits affinity to HAp, however, the drug molecules are bound to the mineral surfaces via electrostatic interactions which results in limited loading content and can cause a burst release when administered. Therefore, as was discussed herein different strategies including coating/reinforcing with polymers or hybrid systems fabrication are utilized for preventing the burst release kinetics. Though it should be emphasized that HAp as a bone mimetic material is frequently used clinically as a bioactive and biocompatible material supporting the implant's biointegration. Therefore, HAp acting as drug carriers might simultaneously serve as a reservoir for calcium and phosphate ions, necessary for bone homeostasis and mineral formation under in vivo conditions. Thus we are convinced that osteogenic and osteoinductive properties of HAp make them important and still a perspective component of ALN carriers, especially in the combination with biopolymeric hybrids/scaffolds.

Furthermore, the issue of ease of administration is also of great importance, especially taking into account the prevention of osteoporosis or cases that cannot be qualified for conventional surgery. For that reason, delivery systems enabling a non-invasive placement at the site of implantation and local action of the drug seem to present an extremely attractive solution, ensuring suppression of bone resorption and at the same time limiting the systemic side-effects of the therapy. Overall, it should be stressed that the aging processes of developed countries' citizens, combined with an unhealthy lifestyle, including not proper diet and limited physical activity, result in many diseases and injuries of the skeletal system, thus increasing the need for transplants and materials that would provide active supplementation of the resulting tissue defects. Furthermore, curing the early osteoporotic stages that do not qualify for the conventional surgical procedures is also a very important issue that should be taken into consideration. Given the complexity of the natural healing cascade in bone, from inflammation to cell recruitment to osteoblastogenesis and next to remodeling, it is doubtful that delivering a single factor and regulating only one aspect of healing will be sufficient to achieve the tissue repair with the necessary functions. There are several interesting delivery platforms that have been tested for non-ALN bisphosphonates, including but not limited to zeolites, magnesium alloys, and montmorillonite based systems (MMS). However, we believe that an approach based on the elegant combination of structures such as HAp, MOF, or mesoporous silica particles with biopolymeric matrices/scaffolds is particularly promising for the development of carriers for BPs delivery. In such designed systems, it is possible to simultaneously achieve multifunctionality, which concerns both the issues of controlling/tuning drug release and the comprehensive bone healing. Satisfying the growing demand for such multifunctional biomaterials for tissue engineering, possessing specific physical, chemical, and biological properties, faces limitations that create technical problems between laboratory testing and real applications. Hence, the possibility of scale availability, low production cost, and high reproducibility of the designed systems are issues that scientists also have to address.

## Acknowledgments

Authors acknowledge the financial support of The National Centre for Research and Development, Poland, No TANGO-V-A/0001/2021-00.

## Disclosure

The authors report no conflicts of interest in this work.

## References

1. Carlson BM. The skeleton. In: *The Human Body*. Elsevier; 2019:87–110.
2. Gisbert-Garzarán M, Manzano M, Vallet-Regí M. Mesoporous silica nanoparticles for the treatment of complex bone diseases: bone cancer, bone infection and osteoporosis. *Pharmaceutics*. 2020;12(1):83. doi:10.3390/pharmaceutics12010083
3. Compston JE, McClung M, Leslie WD. Osteoporosis. *Lancet*. 2019;393(10169):364–376. doi:10.1016/S0140-6736(18)32112-3
4. Rinonapoli G, Ruggiero C, Meccariello L, Bisaccia M, Ceccarini P, Caraffa A. Osteoporosis in men: a review of an underestimated bone condition. *Int J Mol Sci*. 2021;23:22. doi:10.3390/ijms23010022
5. Kanis JA, Norton N, Harvey NC, et al. SCOPE 2021: a new scorecard for osteoporosis in Europe. *Arch Osteoporos*. 2021;16(1):82. doi:10.1007/s11657-020-00871-9
6. Mora-Raimundo P, Manzano M, Vallet-Regí M. Nanoparticles for the treatment of osteoporosis. *AIMS Bioeng*. 2017;4(2):259–274. doi:10.3934/bioeng.2017.2.259
7. Conley RB, Adib G, Adler RA, et al. Secondary fracture prevention: consensus clinical recommendations from a multistakeholder coalition. *J Bone Miner Res off J Am Soc Bone Miner Res*. 2020;35(1):36–52. doi:10.1002/jbmr.3877
8. Seeman E, Delmas PD. Bone quality — the material and structural basis of bone strength and fragility. *N Engl J Med*. 2006;354(21):2250–2261. doi:10.1056/NEJMra053077
9. Diab DL, Watts NB, Miller PD. Bisphosphonates pharmacology and use in the treatment of osteoporosis. In: *Marcus and Feldman's Osteoporosis*. 5th ed. Academic Press; 2021:1721–1736.
10. Zhao X, Zhu L, Fan C. Sequential alendronate delivery by hydroxyapatite-coated maghemite for enhanced bone fracture healing. *J Drug Deliv Sci Technol*. 2021;66:102761. doi:10.1016/j.jddst.2021.102761
11. Ding N, Liu C, Yao L, et al. Alendronate induces osteoclast precursor apoptosis via peroxisomal dysfunction mediated ER stress. *J Cell Physiol*. 2018;233(9):7415–7423. doi:10.1002/jcp.26587
12. Tu KN, Lie JD, Wan CKV, et al. Osteoporosis: a review of treatment options. *Pharm Ther*. 2018;43(2):13.
13. Furman BL. Alendronate. In: *Reference Module in Biomedical Sciences*. Elsevier; 2016:B9780128012383980000.
14. Khan M, Cheung AM, Khan AA. Drug-related adverse events of osteoporosis therapy. *Endocrinol Metab Clin North Am*. 2017;46(1):181–192. doi:10.1016/j.ecl.2016.09.009
15. Nuti R. Updates on mechanism of action and clinical efficacy of risedronate in osteoporosis. *Clin Cases Miner Bone Metab off J Ital Soc Osteoporos Miner Metab Skelet Dis*. 2014;11(3):208–214.
16. Coffman AA, Basta-Pljakic J, Guerra RM, et al. A bisphosphonate with a low hydroxyapatite binding affinity prevents bone loss in mice after ovariectomy and reverses rapidly with treatment cessation. *JBMR Plus*. 2021;5(4):e10476.
17. Reid DM, Hosking D, Kendler D, et al. A comparison of the effect of alendronate and risedronate on bone mineral density in postmenopausal women with osteoporosis: 24-month results from FACTS-International: FACTS-international year 2. *Int J Clin Pract*. 2008;62(4):575–584. doi:10.1111/j.1742-1241.2008.01704.x
18. Sebba AI, Bonnick SL, Kagan R, et al. Response to therapy with once-weekly alendronate 70 mg compared to once-weekly risedronate 35 mg in the treatment of postmenopausal osteoporosis. *Curr Med Res Opin*. 2004;20(12):2031–2041. doi:10.1185/030079904X16768
19. Rosen CJ, Hochberg MC, Bonnick SL, et al. Treatment with once-weekly alendronate 70 mg compared with once-weekly risedronate 35 mg in women with postmenopausal osteoporosis: a randomized double-blind study. *J Bone Miner Res*. 2004;20(1):141–151. doi:10.1359/JBMR.040920
20. Gagné L, Maizes V. Osteoporosis. In: *Integrative Medicine*. Elsevier; 2018:370–381.
21. Fazil M, Baboota S, Sahni JK, Ameerduzzafar AJ, Ali J. Bisphosphonates: therapeutics potential and recent advances in drug delivery. *Drug Deliv*. 2015;22(1):1–9. doi:10.3109/10717544.2013.870259
22. Barry M, Pearce H, Cross L, Tatullo M, Gaharwar AK. Advances in nanotechnology for the treatment of osteoporosis. *Curr Osteoporos Rep*. 2016;14(3):87–94. doi:10.1007/s11914-016-0306-3
23. Nafee N, Zewail M, Boraie N. Alendronate-loaded, biodegradable smart hydrogel: a promising injectable depot formulation for osteoporosis. *J Drug Target*. 2018;26(7):563–575. doi:10.1080/1061186X.2017.1390670
24. Horikawa A, Miyakoshi N, Shimada Y, Sugimura Y, Kodama H. A comparative study between intravenous and oral alendronate administration for the treatment of osteoporosis. *SpringerPlus*. 2015;4(1):675. doi:10.1186/s40064-015-1474-9
25. Yasmin F, Chen X, Eames B. Effect of process parameters on the initial burst release of protein-loaded alginate nanospheres. *J Funct Biomater*. 2019;10(3):42. doi:10.3390/jfb10030042
26. Huang X, Brazel CS. On the importance and mechanisms of burst release in matrix-controlled drug delivery systems. *J Controlled Release*. 2001;73(2–3):121–136. doi:10.1016/S0168-3659(01)00248-6
27. Bose S, Vu AA, Emshadi K, Bandyopadhyay A. Effects of polycaprolactone on alendronate drug release from Mg-doped hydroxyapatite coating on titanium. *Mater Sci Eng C*. 2018;88:166–171. doi:10.1016/j.msec.2018.02.019
28. Kanis JA, Kanis JA. Assessment of fracture risk and its application to screening for postmenopausal osteoporosis: synopsis of a WHO report. *Osteoporos Int*. 1994;4(6):368–381. doi:10.1007/BF01622200
29. Teitelbaum SL. Bone Resorption by Osteoclasts. *Science*. 2000;289(5484):1504–1508. doi:10.1126/science.289.5484.1504
30. Kryśkiewicz E, Lorenc RS. Mechanisms of action of anticatabolic drugs used in osteoporosis therapy. *Pol J Endocrinol*. 2009;60(2):134–144.
31. Pogoda P, Priemel M, Rueger JM, Amling M. Bone remodeling: new aspects of a key process that controls skeletal maintenance and repair. *Osteoporos Int*. 2005;16(S02):S18–S24. doi:10.1007/s00198-004-1787-y
32. Boivin G, Meunier PJ. Changes in bone remodeling rate influence the degree of mineralization of bone. *Connect Tissue Res*. 2002;43(2–3):535–537. doi:10.1080/03008200290000934
33. Viguet-Carrin S, Garnero P, Delmas PD. The role of collagen in bone strength. *Osteoporos Int*. 2006;17(3):319–336. doi:10.1007/s00198-005-2035-9
34. Billington EO, Reid IR. Pathogenesis of osteoporosis. In: *Encyclopedia of Endocrine Diseases*. Elsevier; 2019:222–232.
35. Russell RGG. Bisphosphonates: the first 40 years. *Bone*. 2011;49(1):2–19. doi:10.1016/j.bone.2011.04.022
36. Sinha PS, Rosen HN. Clinical pharmacology of the bisphosphonates. In: *Reference Module in Biomedical Sciences*. Elsevier; 2019: B9780128012383113000.

37. Kuźnik A, Pażdździerniak-Holewa A, Jewula P, Kuźnik N. Bisphosphonates—much more than only drugs for bone diseases. *Eur J Pharmacol*. 2020;866:172773. doi:10.1016/j.ejphar.2019.172773
38. Manzano M, Colilla M, Vallet-Regí M. Drug delivery from ordered mesoporous matrices. *Expert Opin Drug Deliv*. 2009;6(12):1383–1400. doi:10.1517/17425240903304024
39. Zeng Y, Hoque J, Varghese S. Biomaterial-assisted local and systemic delivery of bioactive agents for bone repair. *Acta Biomater*. 2019;93:152–168. doi:10.1016/j.actbio.2019.01.060
40. Boanini E, Torricelli P, Gazzano M, Giardino R, Bigi A. Alendronate–hydroxyapatite nanocomposites and their interaction with osteoclasts and osteoblast-like cells. *Biomaterials*. 2008;29(7):790–796. doi:10.1016/j.biomaterials.2007.10.040
41. Russell R. Determinants of structure–function relationships among bisphosphonates. *Bone*. 2007;40(5):S21–S25. doi:10.1016/j.bone.2007.03.002
42. Russell RGG. Bisphosphonates: mode of action and pharmacology. *Pediatrics*. 2007;119(Supplement 2):S150–S162. doi:10.1542/peds.2006-2023H
43. Eastell R. Osteoporosis. *Medicine*. 2013;41(10):586–591. doi:10.1016/j.mpmed.2013.07.014
44. Chamundeswari M, Jeslin J, Verma ML. Nanocarriers for drug delivery applications. *Environ Chem Lett*. 2019;17(2):849–865. doi:10.1007/s10311-018-00841-1
45. Miladi K, Sfar S, Fessi H, Elaissari A. Encapsulation of alendronate sodium by nanoprecipitation and double emulsion: from preparation to in vitro studies. *Ind Crops Prod*. 2015;72:24–33. doi:10.1016/j.indcrop.2015.01.079
46. Miladi K, Sfar S, Fessi H, Elaissari A. Enhancement of alendronate encapsulation in chitosan nanoparticles. *J Drug Deliv Sci Technol*. 2015;30:391–396. doi:10.1016/j.jddst.2015.04.007
47. Klara J, Marczak A, Łatkiewicz A, Horak W, Lewandowska-Łańcucka J. Lysine-functionalized chondroitin sulfate improves the biological properties of collagen/chitosan-based injectable hydrogels. *Int J Biol Macromol*. 2022;202:318–331. doi:10.1016/j.ijbiomac.2022.01.026
48. Dong J, Tao L, Abourehab MAS, Hussain Z. Design and development of novel hyaluronate-modified nanoparticles for combo-delivery of curcumin and alendronate: fabrication, characterization, and cellular and molecular evidences of enhanced bone regeneration. *Int J Biol Macromol*. 2018;116:1268–1281. doi:10.1016/j.ijbiomac.2018.05.116
49. Moradikhah F, Doosti-Telgerd M, Shabani I, Soheil S, Dolatyar B, Seyedjafari E. Microfluidic fabrication of alendronate-loaded chitosan nanoparticles for enhanced osteogenic differentiation of stem cells. *Life Sci*. 2020;254:117768. doi:10.1016/j.lfs.2020.117768
50. Farbod K, Diba M, Zinkevich T, et al. Gelatin nanoparticles with enhanced affinity for calcium phosphate. *Macromol Biosci*. 2016;16(5):717–729. doi:10.1002/mabi.201500414
51. Lewandowska-Łańcucka J, Mystek K, Mignon A, Van Vlierbergh S, Łatkiewicz A, Nowakowska M. Alginate- and gelatin-based bioactive photocross-linkable hybrid materials for bone tissue engineering. *Carbohydr Polym*. 2017;157:1714–1722. doi:10.1016/j.carbpol.2016.11.051
52. Xu W, Zhao R, Wu T, Li G, Wei K, Wang L. Biodegradable calcium carbonate/mesoporous silica/poly(lactic-glycolic acid) microspheres scaffolds with osteogenesis ability for bone regeneration. *RSC Adv*. 2021;11(9):5055–5064. doi:10.1039/D0RA09958A
53. Choi SW, Kim JH. Design of surface-modified poly(d,l-lactide-co-glycolide) nanoparticles for targeted drug delivery to bone. *J Controlled Release*. 2007;122(1):24–30. doi:10.1016/j.jconrel.2007.06.003
54. Cohen-Sela E, Chorny M, Koroukhov N, Danenberg HD, Golomb G. A new double emulsion solvent diffusion technique for encapsulating hydrophilic molecules in PLGA nanoparticles. *J Controlled Release*. 2009;133(2):90–95. doi:10.1016/j.jconrel.2008.09.073
55. Cenni E, Granchi D, Avnet S, et al. Biocompatibility of poly(d,l-lactide-co-glycolide) nanoparticles conjugated with alendronate. *Biomaterials*. 2008;29(10):1400–1411. doi:10.1016/j.biomaterials.2007.12.022
56. Jing C, Li B, Tan H, et al. Alendronate-decorated nanoparticles as bone-targeted alendronate carriers for potential osteoporosis treatment. *ACS Appl Bio Mater*. 2021;4(6):4907–4916. doi:10.1021/acsabm.1c00199
57. Jing C, Chen S, Bhatia SS, et al. Bone-targeted polymeric nanoparticles as alendronate carriers for potential osteoporosis treatment. *Polym Test*. 2022;110:107584. doi:10.1016/j.polymertesting.2022.107584
58. Hosny KM, Santos HA. Alendronate sodium as enteric coated solid lipid nanoparticles; preparation, optimization, and in vivo evaluation to enhance its oral bioavailability. *PLoS One*. 2016;11(5):e0154926. doi:10.1371/journal.pone.0154926
59. Das T, Venkatesh MP, Pramod Kumar TM, Koland M. SLN based alendronate in situ gel as an implantable drug delivery system – a full factorial design approach. *J Drug Deliv Sci Technol*. 2020;55:101415. doi:10.1016/j.jddst.2019.101415
60. Abd El-Hamid BN, Swarnakar NK, Soliman GM, Attia MA, Pauletti GM. High payload nanostructured lipid carriers fabricated with alendronate/polyethyleneimine ion complexes. *Int J Pharm*. 2018;535(1–2):148–156. doi:10.1016/j.ijpharm.2017.10.064
61. Karabasz A, Szuwarzyński M, Nowakowska M, Bzowska M, Lewandowska-Łańcucka J. Stabilization of liposomes with silicone layer improves their elastomechanical properties while not compromising biological features. *Colloids Surf B Biointerfaces*. 2020;195:111272. doi:10.1016/j.colsurfb.2020.111272
62. Han HK, Shin HJ, Ha DH. Improved oral bioavailability of alendronate via the mucoadhesive liposomal delivery system. *Eur J Pharm Sci*. 2012;46(5):500–507. doi:10.1016/j.ejps.2012.04.002
63. Hosny KM, Ahmed OAA, Al-Abdali RT. Enteric-coated alendronate sodium nanoliposomes: a novel formula to overcome barriers for the treatment of osteoporosis. *Expert Opin Drug Deliv*. 2013;10(6):741–746. doi:10.1517/17425247.2013.799136
64. Wang Q, Huang JY, Li HQ, et al. Recent advances on smart TiO<sub>2</sub> nanotube platforms for sustainable drug delivery applications. *Int J Nanomedicine*. 2016;12:151–165. doi:10.2147/IJN.S117498
65. Shen X, Ma P, Hu Y, et al. Alendronate-loaded hydroxyapatite-TiO<sub>2</sub> nanotubes for improved bone formation in osteoporotic rabbits. *J Mater Chem B*. 2016;4(8):1423–1436. doi:10.1039/C5TB01956G
66. Dlamini N, Mukaya HE, Van Zyl RL, Chen CT, Zeevaart RJ, Mbianda XY. Synthesis, characterization, kinetic drug release and anticancer activity of bisphosphonates multi-walled carbon nanotube conjugates. *Mater Sci Eng C*. 2019;104:109967. doi:10.1016/j.msec.2019.109967
67. Nikfar Z, Shariatinia Z. Phosphate functionalized (4,4)-armchair CNTs as novel drug delivery systems for alendronate and etidronate anti-osteoporosis drugs. *J Mol Graph Model*. 2017;76:86–105. doi:10.1016/j.jmgm.2017.06.021
68. Lee D, Heo DN, Kim HJ, et al. Inhibition of osteoclast differentiation and bone resorption by bisphosphonate-conjugated gold nanoparticles. *Sci Rep*. 2016;6(1):27336. doi:10.1038/srep27336
69. Ryu TK, Kang RH, Jeong KY, et al. Bone-targeted delivery of nanodiamond-based drug carriers conjugated with alendronate for potential osteoporosis treatment. *J Controlled Release*. 2016;232:152–160. doi:10.1016/j.jconrel.2016.04.025

70. Chauhan S, Jain N, Nagaich U. Nanodiamonds with powerful ability for drug delivery and biomedical applications: recent updates on in vivo study and patents. *J Pharm Anal.* 2020;10(1):1–12. doi:10.1016/j.jpha.2019.09.003
71. Munir MU, Salman S, Javed I, et al. Nano-hydroxyapatite as a delivery system: overview and advancements. *Artif Cells Nanomedicine Biotechnol.* 2021;49(1):717–727. doi:10.1080/21691401.2021.2016785
72. Ravanbakhsh M, Labbaf S, Karimzadeh F, Pinna A, Houreh AB, Nasr-Esfahani MH. Mesoporous bioactive glasses for the combined application of osteosarcoma treatment and bone regeneration. *Mater Sci Eng C.* 2019;104:109994. doi:10.1016/j.msec.2019.109994
73. Bosco R, Iafisco M, Tampieri A, Jansen JA, Leeuwenburgh SCG, van den Beucken JJ. Hydroxyapatite nanocrystals functionalized with alendronate as bioactive components for bone implant coatings to decrease osteoclastic activity. *Appl Surf Sci.* 2015;328:516–524. doi:10.1016/j.apsusc.2014.12.072
74. Hwang SJ, Lee JS, Ryu TK, et al. Alendronate-modified hydroxyapatite nanoparticles for bone-specific dual delivery of drug and bone mineral. *Macromol Res.* 2016;24(7):623–628. doi:10.1007/s13233-016-4094-5
75. Sharma N, Purwar N, Gupta PC. Microspheres as drug carriers for controlled drug delivery: a review. *Int J Pharm Sci Res.* 2015;6(12):4103–4112. doi:10.13040/IJPSR.0975-8232.6(10).4103-12
76. Siepmann J, Siepmann F. Microparticles Used as Drug Delivery Systems. In: Richtering W, editor. *Smart Colloidal Materials. Progress in Colloid and Polymer Science.* Vol. 133. Springer Berlin Heidelberg; 2006:15–21.
77. Chen S, Guo R, Xie C, Liang Q, Xiao X. Biomimetic mineralization of nanocrystalline hydroxyapatites on aminated modified polylactic acid microspheres to develop a novel drug delivery system for alendronate. *Mater Sci Eng C.* 2020;110:110655. doi:10.1016/j.msec.2020.110655
78. Yang H, Gao H, Wang Y. Hollow hydroxyapatite microsphere: a promising carrier for bone tissue engineering. *J Microencapsul.* 2016;33(5):421–426. doi:10.1080/02652048.2016.1202347
79. Bae J, Park JW. Preparation of an injectable depot system for long-term delivery of alendronate and evaluation of its anti-osteoporotic effect in an ovariectomized rat model. *Int J Pharm.* 2015;480(1–2):37–47. doi:10.1016/j.ijpharm.2015.01.020
80. Wei P, Yuan Z, Jing W, et al. Strengthening the potential of biomimetic microspheres in enhancing osteogenesis via incorporating alendronate. *Chem Eng J.* 2019;368:577–588. doi:10.1016/j.cej.2019.02.020
81. Vallet-Regí M, Balas F, Arcos D. Mesoporous materials for drug delivery. *Angew Chem Int Ed.* 2007;46(40):7548–7558. doi:10.1002/anie.200604488
82. Narayan R, Nayak UY, Raichur AM, Garg S. Mesoporous silica nanoparticles: a comprehensive review on synthesis and recent advances. *Pharmaceutics.* 2018;10(3):E118. doi:10.3390/pharmaceutics10030118
83. Balas F, Manzano M, Horcajada P, Vallet-Regí M. Confinement and controlled release of bisphosphonates on ordered mesoporous silica-based materials. *J Am Chem Soc.* 2006;128(25):8116–8117. doi:10.1021/ja062286z
84. Colilla M, Izquierdo-Barba I, Vallet-Regí M. Phosphorus-containing SBA-15 materials as bisphosphonate carriers for osteoporosis treatment. *Microporous Mesoporous Mater.* 2010;135(1–3):51–59. doi:10.1016/j.micromeso.2010.06.010
85. Cicco SR, Vona D, Leone G, et al. In vivo functionalization of diatom biosilica with sodium alendronate as osteoactive material. *Mater Sci Eng C.* 2019;104:109897.
86. Saha D, Spurri A, Chen J, Hensley DK. Controlled release of alendronate from nitrogen-doped mesoporous carbon. *Microporous Mesoporous Mater.* 2016;229:8–13. doi:10.1016/j.micromeso.2016.04.014
87. Zhu M, Shi J, He Q, Zhang L, Chen F, Chen Y. An emulsification–solvent evaporation route to mesoporous bioactive glass microspheres for bisphosphonate drug delivery. *J Mater Sci.* 2012;47(5):2256–2263. doi:10.1007/s10853-011-6037-z
88. Wang Y, Yan J, Wen N, et al. Metal-organic frameworks for stimuli-responsive drug delivery. *Biomaterials.* 2020;230:119619. doi:10.1016/j.biomaterials.2019.119619
89. Xue Z, Zhu M, Dong Y, et al. An integrated targeting drug delivery system based on the hybridization of graphdiyne and MOFs for visualized cancer therapy. *Nanoscale.* 2019;11(24):11709–11718. doi:10.1039/C9NR02017A
90. Vassaki M, Papanthanasios KE, Hadjicharalambous C, et al. Self-sacrificial MOFs for ultra-long controlled release of bisphosphonate anti-osteoporotic drugs. *Chem Commun.* 2020;56(38):5166–5169. doi:10.1039/D0CC00439A
91. Al-Baadani MA, Xu L, Hii Ru Yie K, et al. In situ preparation of alendronate-loaded ZIF-8 nanoparticles on electrospun nanofibers for accelerating early osteogenesis in osteoporosis. *Mater Des.* 2022;217:110596. doi:10.1016/j.matdes.2022.110596
92. Zheng X, Zhang Y, Zou L, et al. Robust ZIF-8/alginate fibers for the durable and highly effective antibacterial textiles. *Colloids Surf B Biointerfaces.* 2020;193:111127. doi:10.1016/j.colsurfb.2020.111127
93. Panzavolta S, Torricelli P, Bracci B, Fini M, Bigi A. Alendronate and Pamidronate calcium phosphate bone cements: setting properties and in vitro response of osteoblast and osteoclast cells. *J Inorg Biochem.* 2009;103(1):101–106. doi:10.1016/j.jinorgbio.2008.09.012
94. Yang WK, Chang EJ, Lee WK. Alendronate–calcium phosphate hybrid films promoted the osteoblast differentiation and inhibited osteoclastogenic activity. *J Ind Eng Chem.* 2015;27:391–397. doi:10.1016/j.jiec.2015.01.019
95. Bigi A, Boanini E. Calcium phosphates as delivery systems for bisphosphonates. *J Funct Biomater.* 2018;9(1):6. doi:10.3390/jfb9010006
96. Forte L, Torricelli P, Boanini E, Gazzano M, Fini M, Bigi A. Antiresorptive and anti-angiogenic octacalcium phosphate functionalized with bisphosphonates: an in vitro tri-culture study. *Acta Biomater.* 2017;54:419–428. doi:10.1016/j.actbio.2017.02.040
97. Panzavolta S, Torricelli P, Bracci B, Fini M, Bigi A. Functionalization of biomimetic calcium phosphate bone cements with alendronate. *J Inorg Biochem.* 2010;104(10):1099–1106. doi:10.1016/j.jinorgbio.2010.06.008
98. Dolci LS, Panzavolta S, Albertini B, et al. Spray-congealed solid lipid microparticles as a new tool for the controlled release of bisphosphonates from a calcium phosphate bone cement. *Eur J Pharm Biopharm.* 2018;122:6–16. doi:10.1016/j.ejpb.2017.10.002
99. van Houdt CIA, Gabbai-Armelin PR, Lopez-Perez PM, et al. Alendronate release from calcium phosphate cement for bone regeneration in osteoporotic conditions. *Sci Rep.* 2018;8(1):15398. doi:10.1038/s41598-018-33692-5
100. Park KW, Yun YP, Kim S, Song HR. The effect of alendronate loaded biphasic calcium phosphate scaffolds on bone regeneration in a rat tibial defect model. *Int J Mol Sci.* 2015;16(11):26738–26753. doi:10.3390/ijms161125982
101. Ambrose CG, Clanton TO. Bioabsorbable implants: review of clinical experience in orthopedic surgery. *Ann Biomed Eng.* 2004;32(1):171–177. doi:10.1023/B:ABME.0000007802.59936.fc
102. Giannoudis PV, Schneider E. Principles of fixation of osteoporotic fractures. *J Bone Joint Surg Br.* 2006;88-B(10):1272–1278. doi:10.1302/0301-620X.88B10.17683

103. Hur W, Park M, Lee JY, et al. Bioabsorbable bone plates enabled with local, sustained delivery of alendronate for bone regeneration. *J Controlled Release*. 2016;222:97–106. doi:10.1016/j.jconrel.2015.12.007
104. Boanini E, Torricelli P, Forte L, et al. Antiresorption implant coatings based on calcium alendronate and octacalcium phosphate deposited by matrix assisted pulsed laser evaporation. *Colloids Surf B Biointerfaces*. 2015;136:449–456. doi:10.1016/j.colsurfb.2015.09.044
105. Zheng D, Neoh KG, Kang ET. Immobilization of alendronate on titanium via its different functional groups and the subsequent effects on cell functions. *J Colloid Interface Sci*. 2017;487:1–11. doi:10.1016/j.jcis.2016.10.014
106. Bronze-Uhle ES, Dias LFG, Trino LD, Matos AA, de Oliveira RC, Lisboa-Filho PN. Physicochemical bisphosphonate immobilization on titanium dioxide thin films surface by UV radiation for bio-application. *Surf Coat Technol*. 2019;357:36–47. doi:10.1016/j.surfcoat.2018.09.038
107. Larson N, Ghandehari H. Polymeric Conjugates for Drug Delivery. *Chem Mater*. 2012;24(5):840–853. doi:10.1021/cm2031569
108. Viswanathan P, Muralidaran Y, Ragavan G. Chapter 7 - challenges in oral drug delivery: a nano-based strategy to overcome. In: Andronescu E, Grumezescu AM, editors. *Nanostructures for Oral Medicine*. Elsevier; 2017:173–201.
109. Pan H, Sima M, Kopečková P, et al. Biodistribution and pharmacokinetic studies of bone-targeting N-(2-Hydroxypropyl)methacrylamide copolymer-alendronate conjugates. *Mol Pharm*. 2008;5(4):548–558. doi:10.1021/mp800003u
110. Xie H, Chen G, Young RN. Design, synthesis, and pharmacokinetics of a bone-targeting dual-action prodrug for the treatment of osteoporosis. *J Med Chem*. 2017;60(16):7012–7028. doi:10.1021/acs.jmedchem.6b00951
111. Tang A, Qian Y, Liu S, et al. Self-assembling bisphosphonates into nanofibers to enhance their inhibitory capacity on bone resorption. *Nanoscale*. 2016;8(20):10570–10575. doi:10.1039/C6NR00843G
112. Krajcer A, Klara J, Horak W, Lewandowska-Łańcucka J. Bioactive injectable composites based on insulin-functionalized silica particles reinforced polymeric hydrogels for potential applications in bone tissue engineering. *J Mater Sci Technol*. 2022;105:153–163. doi:10.1016/j.jmst.2021.08.003
113. Bai X, Gao M, Syed S, Zhuang J, Xu X, Zhang XQ. Bioactive hydrogels for bone regeneration. *Bioact Mater*. 2018;3(4):401–417. doi:10.1016/j.bioactmat.2018.05.006
114. Yuan W, Li Z, Xie X, Zhang ZY, Bian L. Bisphosphonate-based nanocomposite hydrogels for biomedical applications. *Bioact Mater*. 2020;5(4):819–831. doi:10.1016/j.bioactmat.2020.06.002
115. Narayanaswamy R, Torchilin VP. Hydrogels and their applications in targeted drug delivery. *Molecules*. 2019;24(3):603. doi:10.3390/molecules24030603
116. Posadowska U, Parizek M, Filova E, et al. Injectable nanoparticle-loaded hydrogel system for local delivery of sodium alendronate. *Int J Pharm*. 2015;485(1–2):31–40. doi:10.1016/j.ijpharm.2015.03.003
117. Papatthanasou KE, Turhanen P, Brückner SI, Brunner E, Demadis KD. Smart, programmable and responsive injectable hydrogels for controlled release of cargo osteoporosis drugs. *Sci Rep*. 2017;7(1):4743. doi:10.1038/s41598-017-04956-3
118. Li D, Zhou J, Zhang M, et al. Long-term delivery of alendronate through injectable tetra-PEG hydrogel to promote osteoporosis therapy. *Biomater Sci*. 2020;8(11):3138–3146. doi:10.1039/D0BM00376J
119. Gilarska A, Hinz A, Bzowska M, et al. Addressing the osteoporosis problem—multifunctional injectable hybrid materials for controlling local bone tissue remodeling. *ACS Appl Mater Interfaces*. 2021;13(42):49762–49779. doi:10.1021/acsami.1c17472
120. Mondal T, Sunny MC, Khastgir D, Varma HK, Ramesh P. Poly (l-lactide-co-ε caprolactone) microspheres laden with bioactive glass-ceramic and alendronate sodium as bone regenerative scaffolds. *Mater Sci Eng C*. 2012;32(4):697–706. doi:10.1016/j.msec.2012.01.011
121. Kim SE, Yun YP, Shim KS, Kim HJ, Park K, Song HR. 3D printed alendronate-releasing poly(caprolactone) porous scaffolds enhance osteogenic differentiation and bone formation in rat tibial defects. *Biomed Mater*. 2016;11(5):055005. doi:10.1088/1748-6041/11/5/055005
122. Kim SE, Yun YP, Han YK, et al. Osteogenesis induction of periodontal ligament cells onto bone morphogenic protein-2 immobilized PCL fibers. *Carbohydr Polym*. 2014;99:700–709. doi:10.1016/j.carbpol.2013.08.053
123. Yun YP, Lee JY, Jeong WJ, et al. Improving osteogenesis activity on BMP-2-immobilized PCL fibers modified by the γ-ray irradiation technique. *BioMed Res Int*. 2015;2015:1–10.
124. Yun YP, Kim SJ, Lim YM, et al. The effect of alendronate-loaded polycaprolactone nanofibrous scaffolds on osteogenic differentiation of adipose-derived stem cells in bone tissue regeneration. *J Biomed Nanotechnol*. 2014;10(6):1080–1090. doi:10.1166/jbn.2014.1819
125. Ma X, He Z, Han F, Zhong Z, Chen L, Li B. Preparation of collagen/hydroxyapatite/alendronate hybrid hydrogels as potential scaffolds for bone regeneration. *Colloids Surf B Biointerfaces*. 2016;143:81–87. doi:10.1016/j.colsurfb.2016.03.025
126. Cattalini JP, Roether J, Hoppe A, et al. Nanocomposite scaffolds with tunable mechanical and degradation capabilities: co-delivery of bioactive agents for bone tissue engineering. *Biomed Mater*. 2016;11(6):065003. doi:10.1088/1748-6041/11/6/065003
127. Wu H, Lei P, Liu G, et al. Reconstruction of large-scale defects with a novel hybrid scaffold made from Poly(L-lactic acid)/Nanohydroxyapatite/alendronate-loaded chitosan microsphere: in vitro and in vivo studies. *Sci Rep*. 2017;7(1):359. doi:10.1038/s41598-017-00506-z
128. Tarafder S, Bose S. Polycaprolactone-coated 3D printed tricalcium phosphate scaffolds for bone tissue engineering: in vitro alendronate release behavior and local delivery effect on in vivo osteogenesis. *ACS Appl Mater Interfaces*. 2014;6(13):9955–9965. doi:10.1021/am501048n
129. Zeng Y, Zhou M, Chen L, et al. Alendronate loaded graphene oxide functionalized collagen sponge for the dual effects of osteogenesis and anti-osteoclastogenesis in osteoporotic rats. *Bioact Mater*. 2020;5(4):859–870. doi:10.1016/j.bioactmat.2020.06.010